

MedRxiv manuscript No.
(will be inserted by the editor)

Basic reproduction number projection for novel pandemics and variants

Ancestral SARS-CoV2 \mathcal{R}_0 projection

Ryan L. Benjamin

Received: date / Accepted: date

Abstract The recently derived Hybrid-Incidence Susceptible-Transmissible-Removed (HI-STR) prototype is a deterministic epidemic compartment model and an alternative to the Susceptible-Infected-Removed (SIR) model prototype. The HI-STR predicts that pathogen transmission depends on host population characteristics including population size, population density and some common host behavioural characteristics.

The HI-STR prototype is applied to the ancestral Severe Acute Respiratory Syndrome Coronavirus 2 (SARS-CoV2) to show that the original estimates of the Coronavirus Disease 2019 (COVID-19) basic reproduction number (\mathcal{R}_0) for the United Kingdom (UK) could have been projected on the individual states of the United States of America (USA) prior to being detected in the USA.

The Imperial College London (ICL) group's \mathcal{R}_0 estimate for the UK is projected onto each USA state. The difference between these projections and ICL's estimates for USA states is either not statistically significant on the paired student t-test or epidemiologically insignificant.

Projection provides a baseline for evaluating the real-time impact of an intervention. Sensitivity analysis was conducted because of considerable variance in parameter estimates across studies. Although the HI-STR predicts that increasing symptomatic ratio and inherently immune ratio reduce \mathcal{R}_0 , relative to the uncertainty in the estimates of \mathcal{R}_0 for the ancestral SARS-CoV2, the projection is insensitive to the inherently immune ratio and the symptomatic ratio.

R. Benjamin
Johannesburg, South Africa
Tel.: +27-11-242-7268
E-mail: Benjamin.L.Ryan@protonmail.com

Keywords HI-SIR · Projection · SARS-CoV2 · basic reproduction number · COVID-19 · Epidemiology Model Taxonomy · Pandemic · variant of concern

1 Introduction

1.1 Motivation

The coronavirus disease 2019 (COVID-19) pandemic highlighted the need to anticipate the impact of a novel pathogen on healthcare [1–4] or the economy [5, 6]. One of the impact factors is the basic reproduction number (\mathcal{R}_0) – a demographic concept that has been repurposed for infectious disease epidemiology [7–11]. \mathcal{R}_0 represents the average number of susceptible people a host infects in a completely susceptible population whilst that host is in its infected state [12, 13]. Based on \mathcal{R}_0 estimates for COVID19’s causative agent, severe acute respiratory syndrome coronavirus 2 (SARS-CoV2), various categories of predictive [1, 14–17], forecast [18–20] and regression [21–24] models have been constructed to anticipate healthcare system demand.

The COVID-19 pandemic’s infections have been periodic [23–27]. Continuous feedback control loops like prevalence dependent contact rates [28] and intervention fatigue [29] may contribute. Equally, irregular events/pulses like relaxation of previous restrictions, superspreader events and migration [29] result in perturbations in the rate of new infections or the active infections [25]. Cyclical events like seasonal host behaviour or pathogen biology, seasonal migration or waning immunity [27, 29] result in periodic infection perturbations or vibrations [24]. The superposition of these perturbations manifest as pandemic waves [30].

For the COVID-19 pandemic, some subsequent waves of infection have been associated with mutations to the ancestral (wild-type) SARS-CoV2 in some countries [29, 31, 32]. Paradoxically, these distinct variant waves may be consequence of SARS-CoV2’s slow virion mutation rate [33–35]. Even if the virion mutation rate is constant, the time to accumulate the appropriate number of mutations in the appropriate loci of a virion, in a sufficiently gregarious individual, in a sufficiently connected geographical location to collectively constitute a variant of concern (VOC) may not be [35]. Thus the timing and the impact of these these events are treated as random and prediction requires manifestation in at least one region. This manuscript projects the impact of a random event like a novel VOC from a region in which it has manifested to one in which it has not. It proposes that each of SARS-CoV2’s VOCs (with its associated perturbations) can be treated as a pandemic and that COVID-19 is the collective manifestations of these overlapping pandemics [36]. Their distinct clinical manifestations provides justification for this approach [37, 38].

Implicitly each VOC contender is a potential new pandemic [29, 34, 39–41]. Consequently, a new local \mathcal{R}_0 can be projected for that VOC. This local \mathcal{R}_0 represents an upperbound of the challenger VOC's impact in anticipation of it outcompeting and supplanting the incumbent [42]. It is an upperbound because, by definition, a \mathcal{R}_0 assumes complete susceptibility to the new variant.

The hybrid-incidence, susceptible-transmissible-removed (HI-STR) [43] model is a deterministic, compartment model prototype constructed to replace two assumptions of Kermack-McKendrick's susceptible-infectious-removed (SIR) prototype [44–46]. It replaces the assumption that the removal rate is proportional to the size of the infected compartment with the more biologically appropriate assumption that the transmissible period is fixed and, consequently, the removal rate is the same as the infection rate one transmissible period ago [43]. It also replaces Hamer's mass action law with its chemistry precursor – the law of mass action [47]. The latter allows the derivation of a population density dependent \mathcal{R}_0 [21, 22, 43].

The HI-STR model differs from existing compartment models by predicting that \mathcal{R}_0 is not only a pathogen property but also depends on the host population's characteristics – including population-size (N), -density (ρ_n) and behaviour [29, 48]. Here a novel method of foretelling local \mathcal{R}_0 in sufficiently behaviourally-similar, isolated populations is introduced. This method is designated projection. It proposes that, if an estimate of \mathcal{R}_0 exists for an isolated population y (${}^y\widehat{\mathcal{R}}_0$), the projection of this \mathcal{R}_0 onto a sufficiently behaviourally similar isolated population z is given by

$$\frac{{}^z\mathcal{R}_0}{{}^y\widehat{\mathcal{R}}_0} = \sqrt[\mathfrak{B}]{\frac{{}^z\rho_n^2 \times {}^zN}{{}^y\rho_n^2 \times {}^yN}} \quad (1)$$

where \mathfrak{B} is determined by the pathogen's transmission dynamics in that host population.

1.2 Background

The omnipresent SIR compartment model prototype for the temporal evolution of an infectious disease proposes that the individuals of an homogenous population can be grouped into three compartments – susceptible, infected and removed [44–46]. Susceptible implies capable of contracting a pathogen, infected implies capable of replicating and spreading the pathogen and removed refers to either recovery (expulsion of the pathogen and immunity) or death. Additional compartments [1, 49] and stratified or heterogenous populations [50–53] result in more sophisticated deterministic, compartment models.

An infectious epidemiology modelling taxonomy is proposed (Figure 1) to distinguish between foretell's common synonyms [54] in mathematical epidemiology. It is proposed that deterministic, compartment models are a subcategory

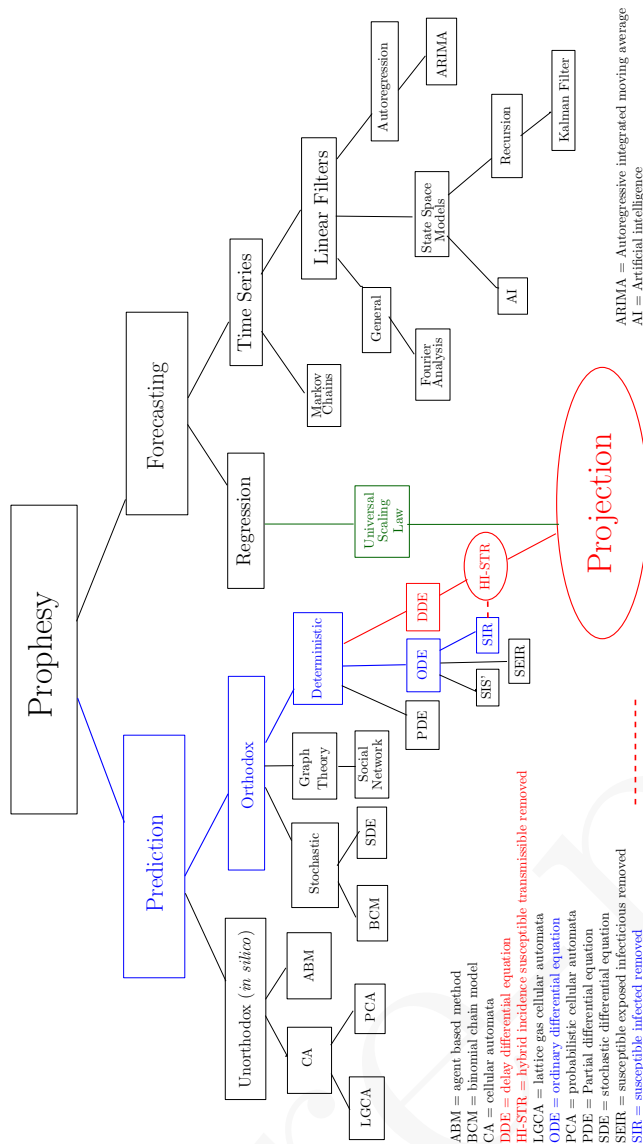


Fig. 1 Epidemiology prophecy taxonomy

of differential equation (DE), orthodox, predictive models. Predictive (mechanistic [55]) models presuppose that phenomena can be explained and that these explanations can be simulated. The orthodox predictive models, consist of a three or four step process of explanation, abstraction into mathematics, the application of a numerical method and *in silico* simulation of the abstraction. The pioneering categories of orthodox models are stochastic and deterministic.

The deterministic compartment models are DE models. The DEs assume an homogenous population and simulate averaged phenomena. The ordinary differential equation (ODE) models only simulate the rate of change of the compartment sizes. Historically, the delay differential equation (DDE) compartment models [56, 57] are an alternative to the exposed (E) compartment of the SEIR ODE model [58–60]. Both the delay term and the E compartment incorporate an incubation period into the SIR prototype. The HI-STR is a DDE model that reduces to an ODE for periodic phenomena [43]. The HI-STR's delay is not due to incubation, it is intended to simulate a constant transmissible period. The transmissible period is another subtle difference from conventional ODE models. Similar to the infectious period, it is the period of time that a host can transmit the disease but it can be limited biologically (*e.g.* the incubation period), behaviourally (*e.g.* isolation, quarantine [61] or hospitalisation) or technologically (*e.g.* face mask or pharmacy). An example of pharmacological restriction to a transmissible period is human immunodeficiency virus (HIV) control where anti-retrovirals (ARVs) substantially reduce viral load and therefore transmissibility. Thus transmissibility may be idealised as a step function under appropriate circumstances [62]. Implicitly, transmissibility is a population characteristic while infectivity is an individual characteristic. Partial differential equation (PDE) models typically model spatial spread as diffusion [63–65]. Algebraic formulae for thresholds like \mathcal{R}_0 and proportion to vaccinate are a consequence of deterministic models

Stochastic, orthodox models translate to binomial chain models (BCM) [66–68] or stochastic differential equation (SDE) models that superimpose uncertainty on ODE models [69–71]. They complement deterministic models with their ability to assign probabilities to outlier events [72] like pathogen extinction. The distribution of the uncertainty is an assumption [73]. Note that the forecasting models (to be described) are also statistical. The distinction is that, like the deterministic models, the stochastic models simulate a theory to prophesize the future while the forecasting models extrapolate the past into the future.

Graph based epidemiological models can be interpreted as an abstraction of an explanation (or a translation) to a branch of mathematics – graph theory [74, 75] – before *in silico* simulation [76–79]. The latter interpretation provides the flexibility of graph theory or the heritage of an established application like social network theory [80–83]. Here graph or network based methods are therefore classified as orthodox predictive methods and ODE alternatives.

The unorthodox predictive methods also presume that phenomena can be explained but the explanation is not translated into mathematics before simulation. Rather, direct *in silico* simulation of the explanation is performed. Thus some graph based implementations can be interpreted as unorthodox [17, 84–87]. Graphs consist of vertices and edges where (for infectious diseases and social networks) the vertices represent individuals and the edges represent

relationships or interactions. Traditionally, the vertices have no geometric interpretation and do not simulate spatial spread [88] but the vertices can be mapped to location [86].

Agent based models (ABM) [6, 16, 89, 90] and cellular automata (CA) [91–93] are spatial, unorthodox, predictive models and PDE alternatives. CA are constructed on a regular lattice and this restriction is removed for ABM [94]. As examples of Artificial Life [95], an agent (or node) acts independently subject to simple rules on the local environment. The collective can prophesize complex phenomena that other predictive methods cannot [96]. These models simulate heterogeneity and mixing [97] but the PDEs that they represent are not apparent [43, 98]. CA can reduce to ODEs [99] and for at least one application (computational fluid dynamics) the PDEs that they represent have been derived [100]. Lattice gas cellular automata (LGCA) [99] and probabilistic (PCA) or stochastic cellular automata (SCA) [92, 93] are subclassifications of CA [43, 98].

Forecasting presumes that phenomena have a recognisable and reproducible pattern. Forecasting fits a curve to a historical pattern and extrapolates the pattern into the foreseeable future [55, 101]. The Fourier theorem states that any curve can be reproduced by an infinite series of superimposed sinusoidal waves [23, 102–106]. Filtering refers to the attenuation (or omission) of frequencies that do not substantively contribute to the signal [23, 102, 107] – resulting in a finite series. In electrical engineering, signal noise is presumed to have high frequency. A low-pass filter (allowing low frequencies to pass) attenuates the noise and smooths the resultant signal [102]. Generally, smoothing is a subset of filtering [102] that attenuates high frequency signals.

The Box-Jenkins forecasting models [108, 109] also fit curves. The prototype is the autoregressive moving average (ARMA) model that forecasts weakly stationary behaviour. The autoregressive integrated moving average (ARIMA) includes trend by differencing to transform the ARIMA model into a stationary model [108–110]. Seasonality (periodicity) can also be incorporated into these time series models [109]. The term autoregression refers to historical data points of a curve being used to estimate the model parameters that predict future values of that same curve [111]. Autocorrelation is a metric of how well past results may foretell future results.

ARIMA models fit a linear combination of a finite number of earlier observations and their differences – parsimonious models [108]. See Mills [111] chapters 6 and 11 for an introduction to non-linear functions. The curve fitting distinguishes the traditional time series models [18, 112, 113] from the artificial intelligence (AI) time series models [112]. Traditional, statistical estimation methods include the maximum likelihood method, the conditional sum of least-squares and the ordinary sum of least-squares [108, 109, 114, 115]. AI is an umbrella term for a collection of methods that searches a space for

an adequate solution. In epidemiology, the AI methods search for parameter combinations that result in adequate curve fitting [19, 116, 117]. Although the parameters are not necessarily optimal, AI excels at non-linear models with or without *a priori* knowledge or understanding of the system's behaviour [118].

State-Space models are a subset of signal-plus-noise problems [107] and are introduced as a form of forecasting [109, 111]. Briefly, an observation (space) equation and a state equation are coupled. Each of these equations has a superimposed uncertainty that is assumed Gaussian [119]. The observation (measurement) equation's independent variable is the signal. In infectious epidemiology; reported new cases, disease mortality [120], waste water serology [121] and combinations thereof are examples of signals. The signal can be a proxy [122, 123] that can be affected by both testing strategy and implementation [120]. For example, South Korea's strategy of significantly increasing access to testing [124] in COVID-19, may have affected the signal quality. Conceivably, universal testing is more effective [125, 126] but less efficient [127] than opportunistic, symptomatic testing [128–131]. Nevertheless, these strategies should converge when asymptomatic infection is rare. Conceivably, a well implemented track-and-trace policy can outperform a poorly promoted/implemented universal testing policy [127, 132, 133].

The unobserved state function is based on *a priori* knowledge of a system's behaviour and can be deterministic [134, 135] or empiric [136, 137]. The measured observation/signal is coupled to an unknown state. Backward and forward recursion approximates a state that corresponds to the signal [107]. The Kalman Filter is a popular recursion method for implementing state-space models [121, 134–139].

The above models require local, disease-specific data for prophesy. Thus, the disease must manifest in that region to determine the model parameters for that region. Cardoso and Gonçalves [21] propose a form for a universal population-size *or* -density dependent scaling law and use regression [101] to determine the parameters for COVID-19. Their approach potentially circumvents the need to determine local modelling parameters locally. Rather, parameters from other centres can be projected – adjusted for local conditions [25]. Figure 2 illustrates the 1 week delay [140] in the stage of spread of the ancestral SARS-CoV2 between the UK and the USA [141]. Given the time dependence of intervention, the universal scaling law may prove more beneficial to regions less connected to the epicentre like India in the COVID-19 example of Figure 2.

Hu *et al* [142] potentially circumvent regression's need for many pre-existing disease centres [21, 25] by repurposing formulae from the kinetic theory of ideal gases to derive population-density dependent contact rates. Hu's contact rates are an alternative to the HI-STR's law of mass action. The HI-STR prototypes' contact rate is population-size *and* -density dependent [43].

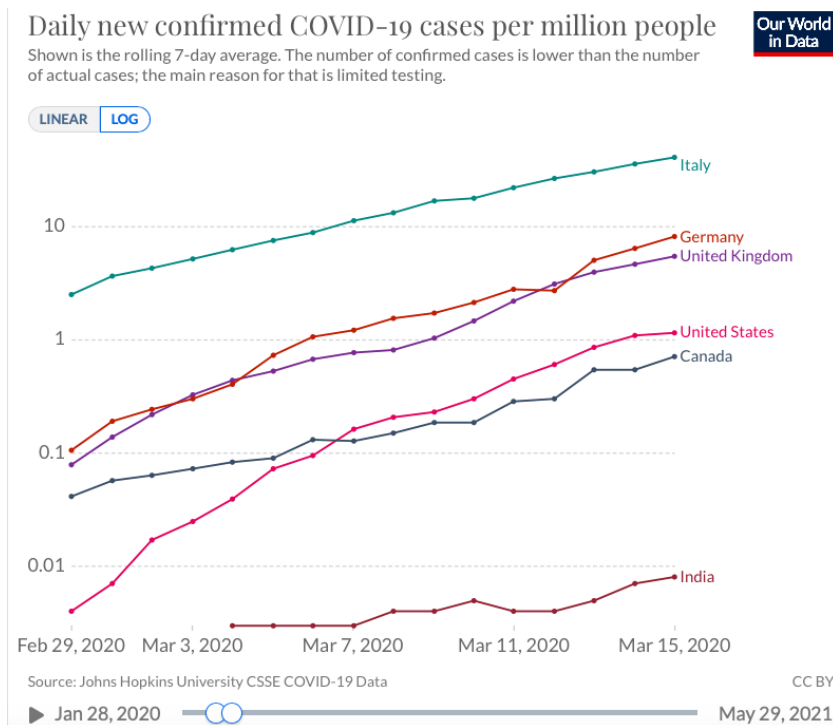


Fig. 2 Delay in confirmed cases per million population by country [141]

2 Methods

The HI-STR prototype is based on the SIR model but replaces 2 assumptions and is formulated for an isolated population on a surface [43]. Thus

1. it is explicit that the model only applies to sufficiently isolated populations,
2. population density is incorporated because it is formulated on a surface and
3. the PDE model formulation problem is replaced by the problem of defining sufficiently isolated populations (SIPs) and sufficient behavioural similarity.

Hamer's mass action law [143] assumption is replaced with the law of mass action [43] – its chemistry precursor [144, 145] – such that the probability density function for a single successful transmission is

$$P(t) = \eta\mu\kappa(\mathbf{x})s(t)\tau(t) \quad (2)$$

where η is an infectious disease-specific variable that reflects avidity, μ is a function of mode of transmission, $\kappa(\mathbf{x})$ is a function of social behaviour, $s(t)$ is the density of susceptible individuals and $\tau(t)$ is the density of hosts capable

of transmitting the pathogen. The total transmissions (including those of secondary hosts) in a population of size $N \gg 1$ and population density ρ_n over the period that the primary host is transmission capable ($\Delta\bar{\tau}$) is shown to be

$$\int_{\Delta\bar{\tau}} \dot{T}(t_0) dt \approx \int_{\Delta\bar{\tau}} \eta\mu\kappa \frac{N^2}{2} s(t_0)\tau(t_0) dt = \int_{\Delta\bar{\tau}} \beta_A \rho_n^2 S(t_0) T(t_0) dt$$

where $S(t)$ is the size of the susceptible population, $T(t)$ is the size of the transmission-capable population and $\beta_A = \frac{\eta\mu\kappa}{2}$ [43].

The SIR prototype's exponential infectious period assumption is replaced with the HI-STR model's more biologically appropriate constant transmission period. This results in the SIR-like DDE model.

$$\begin{aligned} \dot{S}(t) &= -\beta_A \rho_n^2(\mathbf{x}) S(t) T(t) \\ \dot{T}(t) &= \beta_A \rho_n^2(\mathbf{x}) S(t) T(t) - \dot{T}(t - \Delta\bar{\tau}) \\ \dot{R}(t) &= \dot{T}(t - \Delta\bar{\tau}). \end{aligned}$$

Selecting a timescale (the transmissible timescale) where a time unit (Δt) equates to $\Delta\bar{\tau}$ ($1 : \Delta t = 1 : \Delta\bar{\tau}$) renders the delay negligible – reducing the above DDE to an ODE [43].

Exploiting the periodicity of infection opportunity, a second timescale (the rhythmic timescale) is defined as $1 : \Delta t = 1 : \delta t$ where δt is the period of the infection opportunity cycle. For respiratory infectious diseases, δt is the host's sleep-wake cycle (*ie* 1 day). Given that there are \mathfrak{B} units of δt in $\Delta\bar{\tau}$, the number of infections after $\mathfrak{B}\delta t$ is the same as after $\Delta\bar{\tau}$. A binomial expansion is used to show that the ODE in the transmissible timescale reduces to

$$\begin{aligned} \dot{S}(t) &= -\sqrt[\mathfrak{B}]{\beta_A \rho_n^2 N} \frac{S(t) T(t)}{N(\mathbf{x})} \\ \dot{T}(t) &= \sqrt[\mathfrak{B}]{\beta_A \rho_n^2 N} \frac{S(t) T(t)}{N(\mathbf{x})} - \sqrt[\mathfrak{B}]{\tau\alpha} I(t) \\ \dot{R}(t) &= \sqrt[\mathfrak{B}]{\tau\alpha} I(t) \end{aligned}$$

in the rhythmic timescale [43] where $\tau\alpha$ is the infection frequency in the transmissible timescale. The HI-STR model's rhythmic timescale basic reproduction number for SIP z is then [43, 146]

$${}^z_{\rho} \mathcal{R}_0 = \sqrt[\mathfrak{B}]{\frac{\beta_A \times {}^z \rho_n^2 \times {}^z N}{\tau\alpha}}. \quad (3)$$

Both β_A and $\tau\alpha$ are dependent on behavioural characteristics that may be cultural [48, 147]. These are assumed constant for behaviourally-similar populations. There is a subtle difference between Böckh's \mathcal{R}_0 and its rhythmic timescale equivalent, ${}_{\rho} \mathcal{R}_0$, but these are used interchangeably here [43].

Dividing Equation 3 for SIP z by the same for behaviourally-similar SIP y derives Equation 1. It is assumed that the anglophone United Kingdom (UK) and United States of America (USA) have similar concepts of personal space and familiarity with an associated hierarchy of physical interaction rituals [148] such that Equation 1 applies. A metric for behavioural/cultural similarity was not identified. Conceivably, host behaviour could be sufficiently similar across all SIPs. If host behaviour is sufficiently similar across SIPs, then Equation 1 is a universal scaling law (independent of behaviour) and should be compared with Cardoso and Gonçalves' universal scaling law [21] obtained by regression. The UK and USA were selected to increase the likelihood of a successful validation. From Figure 2, projection would have given the most connected states one week's lead time. The ancestral SARS-CoV2 pathogen was selected because transmission dynamics data were available, there was no interference from VOCs and the Imperial College London (ICL) group estimated \mathcal{R}_0 for the ancestral SARS-CoV2 in both the USA and the UK..

The same field- (reported mortality) and estimation methods [140] were used by the ICL group to measure the ancestral SARS-CoV2's \mathcal{R}_0 for the UK [140] and the individual states of the USA [149]. Consequently, using these studies to validate the projection of the UK's \mathcal{R}_0 on to the USA's states avoids biases introduced by different field- and estimation methods. Their semi-mechanistic Bayesian hierarchical model is sensitive to the generation interval [140] but a gamma distribution with mode 6.5 days was used for their $\hat{\mathcal{R}}_0$ for both the UK and the USA states. From Equation 1, the projection onto state z is

$${}^z\mathcal{R}_0 = \sqrt[3]{\frac{{}^z\rho_n^2 \times {}^zN}{{}^{UK}\rho_n^2 \times {}^{UK}N}} \times {}^{UK}\hat{\mathcal{R}}_0. \quad (4)$$

The paired student-t test is used to compare the USA \mathcal{R}_0 estimates (${}^z\hat{\mathcal{R}}_0$) [149] to the UK's projection on z (${}^z\mathcal{R}_0$).

Statistical analysis was conducted in the open-source R Project for statistical computing (<https://www.r-project.org>)

3 Results

The transmission dynamics, distribution of pathology, case fatality rate and other clinical, pathological and epidemiological characteristics associated the ancestral (wild type) SARS-CoV2 are collectively designated COVID-19(wt). Appendix 6.1 demonstrates that the transmissible timescale for COVID-19(wt) is 1 : 9 days and the rhythmic timescale is 1 : 1 day. The ratio of the time units in these timescales (\mathfrak{B}) is 9.

The UK's estimated \mathcal{R}_0 is ${}^{UK}\hat{\mathcal{R}}_0 = 3.8[3.0 - 4.5]$ [140], ${}^{UK}N = 67,886,011$ with ${}^{UK}\rho_n = 280.6 km^{-2}$ in 2020 [150]. Equation 4 projects this ${}^{UK}\hat{\mathcal{R}}_0$ onto

the states of the USA adjusting for each state's population-size and -density. Appendix 6.2 removes any outliers. Figure 3 compares the $\hat{\mathcal{R}}_0$ density distribution [149] of the remaining 40 states to those projected from the UK estimate (${}^{UK}\hat{\mathcal{R}}_0$) [140]. Figure 3(a) projects the median UK estimate (${}^{UK}\hat{\mathcal{R}}_0 = 3.8$) while Figure 3(b) projects ${}^{UK}\hat{\mathcal{R}}_0 = 4.2$. The latter remains within the uncertainty of the UK's $\hat{\mathcal{R}}_0$ estimate [140].

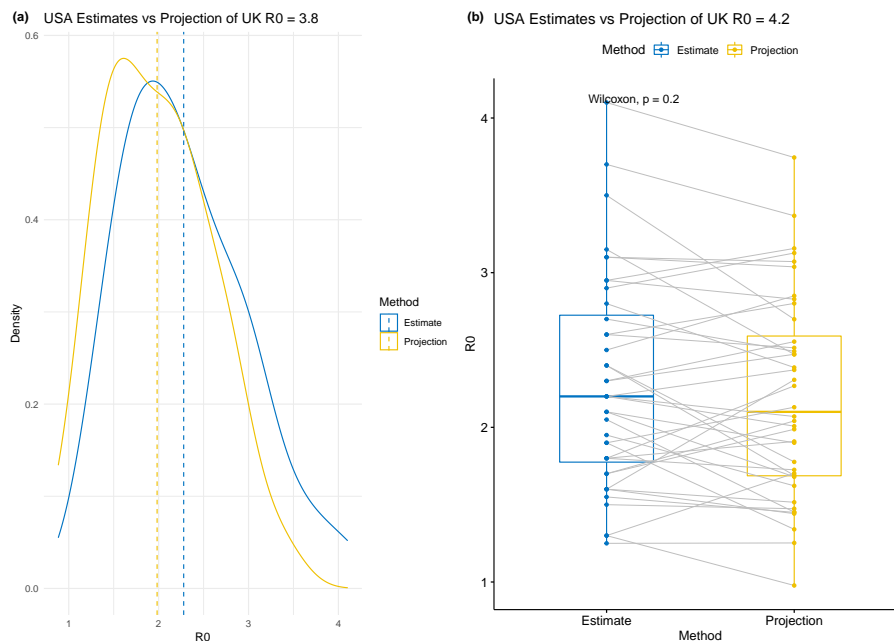


Fig. 3 (a) Density distribution comparison between estimated \mathcal{R}_0 the median estimated \mathcal{R}_0 for the UK projected on to the USA's state (b) Box-and-whisker plot comparison between estimated \mathcal{R}_0 and a UK $\hat{\mathcal{R}}_0 = 4.2$ projected on to the USA's states

Table 1 summarises the results of the paired student t-test comparing the estimated \mathcal{R}_0 s [149] of the 40 USA states (${}^z\hat{\mathcal{R}}_0 : 1 \leq z \leq 40, z \in \mathcal{N}$) to the projections of the ${}^{UK}\hat{\mathcal{R}}_0$ (within the range [3.0 – 4.5]) [140] on to those 40 states.

Of note, for $4.2 \leq {}^{UK}\hat{\mathcal{R}}_0 \leq 4.5$, a statistically significant difference between the estimated and projected \mathcal{R}_0 s does not exist for those 40 states. For $3.0 \leq {}^{UK}\hat{\mathcal{R}}_0 \leq 4.1$, although there is a statistically significant difference between the estimated and projected \mathcal{R}_0 ; this difference is not epidemiologically significant when compared to the uncertainty in ${}^z\hat{\mathcal{R}}_0$ for those states [149].

	Estimated UK basic reproduction number (${}^{UK}\widehat{\mathcal{R}}_0$)					
${}^{UK}\widehat{\mathcal{R}}_0$	3.0	3.4	3.8	4.1	4.2	4.5
p	7×10^{-15}	5×10^{-11}	4×10^{-6}	0.02	0.13	0.24
μ_d	0.7	0.5	0.3	0.1	0.1	-0.1
CI_d	[0.6, 0.8]	[0.4, 0.6]	[0.2, 0.4]	[0.0, 0.25]	[0.0, 0.2]	[-0.2, 0]

Table 1 Comparison of paired student t -test results between estimated and projected basic reproduction numbers in the USA for various UK basic reproduction number estimates. μ_d is mean of differences. CI_d is 95% confidence interval of the differences. $N = 40$.

The model assumes no inherent immunity. Furthermore, the parameter estimates for \mathfrak{B} have considerable variation (Tables 2 and 3). Appendix 6.3 is a sensitivity analysis demonstrating that up to an inherently immune fraction of 50% the change in the ${}^z\mathcal{R}_0$ projections is not significant compared to the uncertainty in ${}^z\mathcal{R}_0$ – Figure 4(b). Similarly, changing the symptomatic fraction does not cause an epidemiologically significant change in \mathcal{R}_0 – Figure 4(a). The infectious and transmissible periods are varied in Figures 4(c) and (d), respectively.

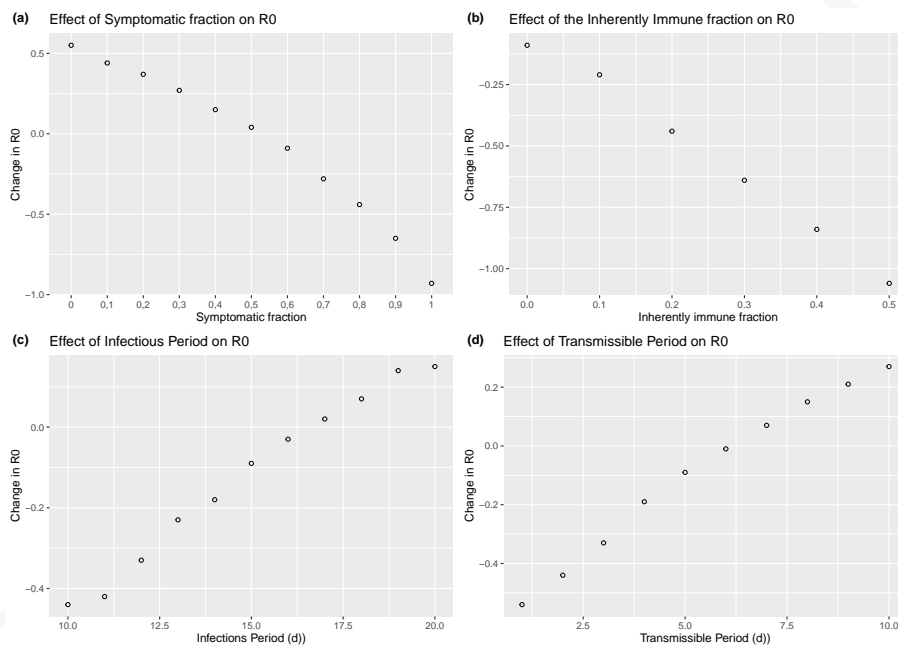


Fig. 4 Sensitivity Analysis for COVID19(wt): (a) Symptomatic fraction (b) Inherently immune fraction (c) Infectious period (d) Transmissible period

Despite the above, the HI-STR predicts that increasing the symptomatic fraction decreases \mathfrak{B} and, consequently, \mathcal{R}_0 by increasing the contribution

of those with a shorter transmissible period (Figure 4(a)). It confirms that increasing the inherently immune fraction reduces \mathcal{R}_0 (Figure 4(b)). As expected, increasing the infectious or transmissible periods increase \mathfrak{B} and therefore \mathcal{R}_0 (Figures 4(c) and (d)).

4 Discussion

Coronavirus disease 2019 (COVID-19) is the umbrella term for the diverse pathological manifestations of severe acute respiratory syndrome coronavirus 2 (SARS-CoV2) and its variants. New variants have the potential to supplant pre-existing variants. Projection provides an efficient method to prophesize variant-specific resource requirements. The hybrid incidence, susceptible-transmissible-removed (HI-STR) has demonstrated that projection can be used to foretell the impact of a pathogen variant (the ancestral SARS-CoV2) on the individual states of the United States of America (USA) provided an estimate exists for the United Kingdom (UK). This was possible because the HI-STR accounts for the effect of population characteristics on the basic reproduction number (\mathcal{R}_0). These regions were selected because it is assumed that the individual states of the USA are sufficiently isolated from each other and because it is assumed that these anglophone regions have sufficient behavioural similarity.

It should be noted that the HI-STR prototype does not include the effect of demography [151] on \mathcal{R}_0 estimation and projection but age-stratified SIR models can be adapted for the HI-STR. Genetically or behaviourally predisposed individuals also represent subpopulations that affect the average transmission period. For COVID-19, diabetics are a subpopulation that are at increased risk of severe disease and death [152,153]. The prototype does not include the effect of the distribution of predisposed subpopulations. Clearly the individual states of the USA are not homogenous but a common set of acceptable public behavioural norms must exist.

Hawaii, Montana, Alaska and Wyoming are among the outliers. The HI-STR projections over-estimate \mathcal{R}_0 for these states. For Hawaii, the sea acts as a natural barrier between SIPs. Because the HI-STR is non-linear, these regions cannot be combined. Combining SIPs artificially increases \mathcal{R}_0 projections. Communities within Alaska, Montana and Wyoming may be sufficiently isolated for them to be treated as SIPs. Conversely, states like New York and Washington, DC may not be sufficiently isolated. Neither the method for averaging \mathcal{R}_0 estimates across SIPs nor the estimation of \mathcal{R}_0 across SIPs is obvious.

This work's motivation is the timeous preparation for the local impact of novel pathogen or new VOC. Implicitly, each variant is being treated as a new pathogen to which the local population is completely susceptible. The SARS-CoV2 variants are sufficiently closely related that both vaccination and

previous infection by the incumbent may confer immunity to the new variant in some individuals. Thus the projection represents an upperbound in which the challenger VOC replaces the incumbent [42]. This model does not address an equilibrium states where VOCs form a mixture [34]. Intuitively and theoretically, the inherently and naturally immune individuals should affect the transmission dynamics of the variant and the transmissible period. Given the uncertainty in the wild type COVID-19 \mathcal{R}_0 estimates, here it was not possible to show that these would have an epidemiologically significant impact.

Intuitively, asymptomatic carriers increase the reproduction number [154]. Uniquely, the HI-STR predicts this phenomenon (See Appendix 6.3) but, given the uncertainty in the SARS-CoV2 ancestral \mathcal{R}_0 estimates, this effect is not epidemiologically significant. For diseases where a correlation exists between symptoms and mortality, an intervention that only converts symptomatic individuals into asymptomatic individuals may reduce mortality. Ironically, the theory predicts that such an intervention will increase \mathcal{R}_0 .

5 Conclusion

When confronting a novel pathogen, the impact of the disease has to be foretold to prepare accordingly. Some of these impacts are the basic reproduction number (a proxy for how fast the disease will spread), mortality and morbidity. Some of the impacts that are beyond the scope of this document are the economic and socio-political instability caused by the disease and the intervention.

The hybrid incidence, susceptible-transmissible-removed (HI-STR) prototype is a deterministic alternative to the susceptible-infectious-removed prototype and its ordinary differential equation (ODE) model derivatives. In principle, it has two advantages over these more mature models – it incorporates population-size and -density in the model, and it includes a social or behavioural component. The latter is controversial but it should be noted that the HI-STR has the flexibility to include a social component in the model. It may be that physical interaction across regions and cultures is sufficiently similar (from an infectious disease perspective) that this variable can be treated as a constant. In the latter case, the HI-STR derives a populations-size *and* -density dependent universal scaling law for \mathcal{R}_0 .

The importance of the capacity to project a \mathcal{R}_0 for a region is that it allows planning and pre-emptive resource allocation. It also provides a location-specific \mathcal{R}_0 (baseline) to evaluate interventions. This manuscript demonstrates that the HI-STR model can project the UK's ancestral SARS-CoV2's \mathcal{R}_0 onto the states of the United States. It must still be demonstrated for other anglophone and non-anglophone regions.

There are 2 parts to the intervention – the intervention policy and the policy implementation. Policies and strategies [155] can only be evaluated retrospectively [156–160] because of unforeseen long-term risks [161–166] and unintended consequences [167–171]. For regions with the same intervention policy, the location-specific \mathcal{R}_0 provides a baseline to compare intervention implementation across those regions.

A weakness that the HI-STR currently shares with the other ODE models is that it does not predict the waves of infection seen with both SARS-CoV2 and the Spanish influenza of 1918 [40]. Models can be constructed with periodic interventions or behaviour resulting in periodic infections [29]. SARS-CoV2 has demonstrated that some of these waves may be due to new variants out-competing incumbents [29]. The HI-STR model does not account for pathogen evolution and random events like VOCs but here it has been demonstrated that such an event can still be projected timeously. Seasonal changes in pathogen biology or behaviour can be incorporated into the avidity term (η) and seasonal changes in host behaviour can be included in the social behaviour term ($\kappa(\mathbf{x})$) of the transmission probability density function (Equation 2). Migration requires a spatial model [40].

The HI-STR predicts that an intervention that only converts symptomatic individuals into asymptomatic individuals will increase \mathcal{R}_0 . A risk that can therefore be foreseen is that, even if the virion mutation rate remains constant [35], an increased \mathcal{R}_0 should increase the pathogen population’s mutation rate.

6 Appendices

6.1 The HI-STR parameters for the ancestral SARS-CoV2

COVID-19 is a collection of clinical symptoms and pathologies [172, 173] assigned to several variants of SARS-CoV2 [174–176]. The heterogeneity of pathology [177, 178] is due to both variable host responses to a variant [179–182], and multiple viral lineages [183, 184], their variants [185, 186] and their mutations [187, 188]. Here COVID-19(wt) will refer to the distribution of pathology, case fatality rate, severity and transmission dynamics of the subset of COVID-19 due to L lineage of the ancestral (wild type) SARS-CoV2 [181] to distinguish it from the corresponding findings of the α (B.1.1.7) [189], β (B.1.351), δ (B.1.617.2) [36, 183] and o (B.1.1.529) [186] variants.

Benjamin [43] defines a time unit in the transmissible timescale as the weighted average of the time a host can transmit a pathogen. The transmission period is limited by viral load in a latent period, recovery, death, pharmacological intervention and behavioural adaptation like quarantine. The weighting is based on the relative proportions of inherently immune ($1 - \sigma$), symptomatic (ψ), asymptomatic ($1 - \psi$), and other subpopulations with distinct transmis-

sion periods.

The assumption is that, for a novel pathogen, when sufficient contact is made between a host and a potential host (in a completely susceptible population) there are 3 possible outcomes. There are inherently immune/resistant individuals (not previously exposed) that will not become infected and therefore have a transmission period of zero [190–192], there are asymptomatic individuals [129,193] that may have the transmission period shortened by clearing the virus [189,194] or prolonged by not isolating [53,195], and the symptomatically infected who will have the transmission shortened by either self-isolation, hospitalisation or death. In principle, each of these group’s transmission periods and transmissibility [194,196] are dependent on the demography [151,195], comorbidities [152,153] and genetic predispositions [197] within that group.

The prevalence of asymptomatic infection has been reviewed [195,198]. Whole population survey’s from 2020 of presumed COVID-19(wt) and a young adult challenge trial [199] are presented in Table 2. The prevalences may re-

<i>n</i>	Infected if tested	Asymptomatic	Population
36	53%	11%	Human challenge trial [199]
3711		17.9%	Diamond Princess Cruise Ship [200]
565	2.3 %	30.8 %	Japanese evacuees from Wuhan [193]
10090		31 %	Seven whole population meta-analyses including Vo’, Italy [198]
5155	2.0 %	42.2 %	Vo’, Italy [201]
3711	19.2 %	46.5 %	Diamond Princess Cruise Ship [202]
1766	59.4 %	47.8 %	Charles de Gaulle Aircraft Carrier [195]
4954	17.3 %	58.4 %	USS Theodore Roosevelt [195]
217	59 %	81.3 %	Cruise Ship Ernest Shackleton [131]

Table 2 Asymptomatic prevalence for COVID-19(wt).

flect demography. The median asymptomatic prevalence of 42.2% will be used further.

The infectious period and infectiousness of these groups have been reviewed [61,196,203,204]. Each study uses viral load as an imperfect proxy for infectiousness [128,204–206]. Lavezzo *et al* [201] shortens the viral particle shedding period by 4 days [128,206] to determine the infectious period because the host continues to shed inactive viral RNA for 4 days before the RT-PCR assays can no longer detect them. Table 3 presents the latent, incubation and infectious periods for the symptomatic and asymptomatic.

The latent period is from infection to sufficient viral shedding for successful transmission. Incubation is from infection to symptom onset. The period of time that a virus is detectable has been shortened by 4 days to obtain the infectious period because of the detectable inactive viral RNA post recovery.. It is

Location (A/n)	Symptomatic				Asymptomatic
	Infectious	Latent	Incubation	Transmissible ($\Delta\tau$)	Infectious (ΔI) [Source]
UK Challenge(2/18)	8 d	2 d	4 d	2 d	8 d [199]
S.Korea (89/303)	13 d			15 d	15.5 d [207]
S.Korea (68/396)	14 d				10.5 d [208]
Gangzhou (0/77)	14 d	5.8 d		6 d	[209]
Wuhan (37/178)	10 d		8 d		15 d [210]
Washington (3/48)	14 d			4 d	18 d [128]

Table 3 Median latent, incubation, infectious and transmissible periods for symptomatic and asymptomatic COVID-19(wt) patients from early 2020. $A = asymptomatic$, $d = days$.

assumed that symptomatic patients self-isolate, are hospitalised or ostracised at symptom onset or within a day thereof. Therefore the transmissible period is the difference between the incubation and latent periods.

In each of these studies there is no demonstrable difference in infectivity between these groups [203, 204, 206, 208]. Table 3 mitigates the bias of retrospective studies [194] by only including whole population studies. Nevertheless each population is unique and not necessarily representative. Of note; there may be small differences in the definition of symptomatic and asymptomatic individuals, different real time reverse transcriptase polymerase chain reaction (RT-PCR) platforms were used and different cycle count thresholds used.

The proportion of naturally immune or resistant ($1 - \sigma$) is unknown. Although the UK challenge trial [199] is prospective, neither the sample nor the inoculum are necessarily representative. It is assumed that the naturally immune and resistant are negligible ($\sigma = 1$). In summary, 42.2% are asymptomatic carriers with a 15 day transmission period ($\Delta\tau$) and the symptomatic 57.8% have $\Delta\tau = 5$ days. Consequently, the weighted average transmission period is $\Delta\bar{\tau} = 9$ days and the transmissible times scale is 1 : 9 days.

Periodic human behaviour is the result of superimposed daily, weekly, monthly and annual cycles. For infectious diseases, the rhythmic timescale is determined by the periodicity of transmission opportunity. For airborne diseases like COVID-19, the dominant cycle is diurnal with maximum transmission opportunity during day time social interactions and reduces to a minimum while sleeping. The periodic timescale ($1 : \delta t$) for COVID-19 is thus 1 : 1 day.

The \mathfrak{B} constant in Equations 1 and 3 is the ratio of a unit of time in transmissible times scale ($\Delta\bar{\tau}$) to a time unit in the rhythmic timescale (δt). Thus, for COVID-19(wt), $\mathfrak{B} = 9$.

6.2 States of the USA basic reproduction number outliers

Re-arranging Equation 3, substituting the median reproduction numbers estimates (${}^z\hat{\mathcal{R}}_0$) for the $1 \leq z \leq 51$ states of the USA [149] and, the population-sizes (zN) and -densities (${}^z\rho_n$) for these states [150] allows one to determine the proportionality constant ($M = \frac{\hat{\beta}_A}{\tau\alpha}$) in

$${}^z\hat{\mathcal{R}}_0^{\mathfrak{B}} = M \times {}^zN \times {}^z\rho_n^2 \quad \iff \quad M = \frac{{}^z\hat{\mathcal{R}}_0^{\mathfrak{B}}}{{}^zN \times {}^z\rho_n^2}.$$

Figure 5 (the density distribution for M) identifies 6 outliers. The median

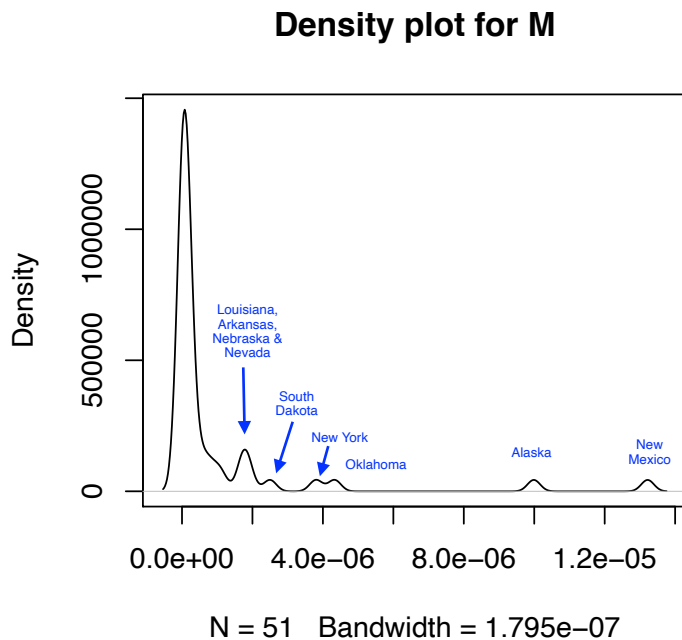


Fig. 5 Population density distribution of M in $\mathcal{R}_0^{\mathfrak{B}} = M \times \rho_n^2 N$

[IQR] of the proportionality constant M is $1.1 \times 10^{-7} [3.4 \times 10^{-8}, 6.2 \times 10^{-7}]$.

New Mexico, Alaska, Oklahoma, New York, South Dakota and Louisiana are removed from further analysis.

The relative error between the predicted basic reproductive (${}^z\mathcal{R}_0$) and ${}^z\hat{\mathcal{R}}_0$:

$$E := \frac{{}^z\mathcal{R}_0 - {}^z\hat{\mathcal{R}}_0}{{}^z\hat{\mathcal{R}}_0} \quad \text{where} \quad {}^z\mathcal{R}_0 = M \times {}^zN \times {}^z\rho_n,$$

is assumed to have a Gaussian distribution about a mean of 0. The Median [IQR] of E is $-0.02[-0.17, 0.05]$. Figure 6 is the density distribution of the rela-

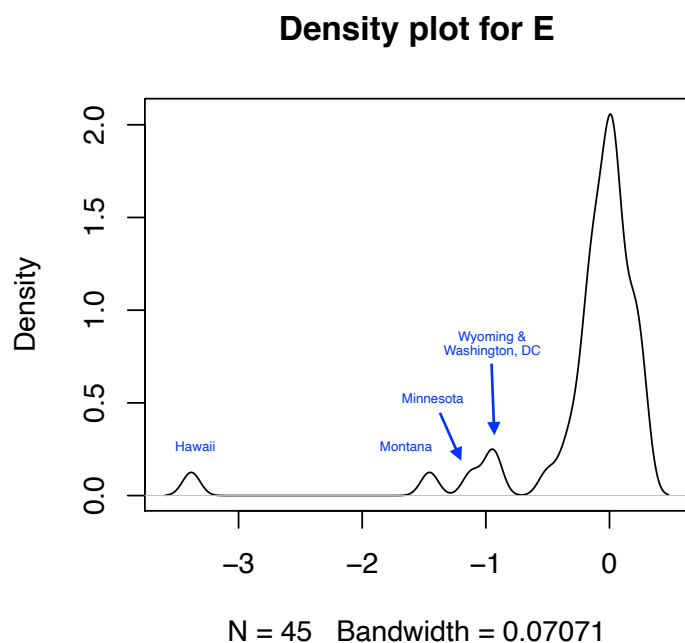


Fig. 6 Population density distribution of E , the relative error between the observed and predicted basic reproductive numbers

tive error between the predicted and measured reproductive numbers. Hawaii, Montana, Minnesota, Wyoming and Washington DC are removed as outliers.

Figure 7 compares the density distributions of $\hat{\mathcal{R}}_0$ and \mathcal{R}_0 for the remaining 40 states of the USA and demonstrates that the relative error, E , is normally distributed. The Shapiro-Wilk test on E could not exclude normality ($p =$

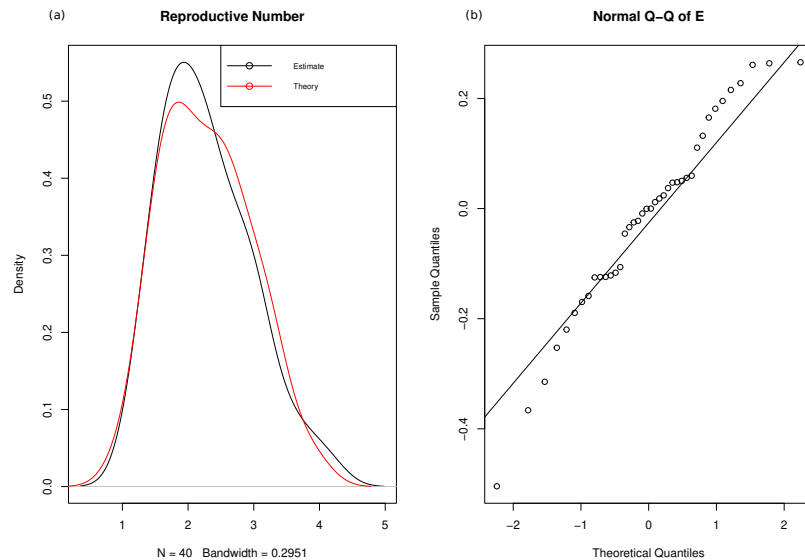


Fig. 7 (a) Comparison of the theoretical and estimated $\rho \mathcal{R}_0$, (b) Demonstration of the normality of the relative error E

0.31).

6.3 Sensitivity analysis – impact of asymptomatic ratio

The ratio of the time units in the transmissible timescale to the time units in the rhythmic timescale (\mathfrak{B}) translates to the average transmissible period ($\Delta\bar{\tau}$) for the special case where the time units in the rhythmic timescale (δt) = 1. For this special case, \mathfrak{B} is dependent on 4 variables

$$\begin{aligned} \mathfrak{B} &= \sigma(1 - \psi) \times \Delta I + \sigma\psi \times \Delta\tau + (1 - \sigma) \times 0 \\ &= \sigma(1 - \psi) \times \Delta I + \sigma\psi \times \Delta\tau = \Delta\bar{\tau} \quad \text{where } \delta t = 1, \end{aligned}$$

σ is the non-immune or susceptible portion of the population, $1 - \sigma$ is the immune portion that cannot be infected, ψ is the portion of σ that will be symptomatic if infected, $1 - \psi$ is the proportion that will be asymptomatic if

infected, ΔI is the infectious period and $\Delta\tau$ is the transmissible period.

Thus far, this manuscript has assumed that $\sigma = 1$ while Tables 2 and 3 demonstrate the considerable variance in the estimates of ψ and ΔI and $\Delta\tau$, respectively. Figure 4 is a sensitivity analysis depicting the effect of changes in:

- (a) the symptomatic fraction (ψ) when the inherently immune fraction ($1 - \sigma$), infectious period (ΔI) and transmissible period ($\Delta\tau$) are held constant at 0; 15 days and 5 days, respectively;
- (b) the inherently immune fraction ($1 - \sigma$) is varied from 0 to 0.5 with $\psi = 0.6$, $\Delta I = 15$ days and $\Delta\tau = 5$ days. The distribution of the constants M and E deviate from normality for $\psi > 0.5$;
- (c) infectious period (ΔI) with $1 - \sigma = 0$, $\psi = 0.6$ and $\Delta\tau = 5$ days and
- (d) transmissible period ($\Delta\tau$) with $1 - \sigma = 0$, $\psi = 0.6$ and $\Delta I = 15$ days

on the difference between UK's projection of $\hat{\mathcal{R}}_0 = 4.2$ onto the USA states and the USA estimates of \mathcal{R}_0 - projection - estimate.

As expected, increasing the symptomatic fraction (ψ) or the inherently immune fraction ($1 - \sigma$) reduced \mathcal{R}_0 . Of note, relative to the estimates and the uncertainties in these estimates [149] the reduction in \mathcal{R}_0 is epidemiologically insignificant over the domains investigated. The E distribution deviates from normality on the Shapiro-Wilk's test for inherently immune ratios greater than 40% and visibly for ratios greater than 50%.

Increasing either the infectious period (ΔI) or the transmissible period ($\Delta\tau$) increased \mathcal{R}_0 . Again, relative to the estimates and the uncertainty in these estimates [149], the increase in \mathcal{R}_0 is epidemiologically insignificant for wild type COVID19.

7 Declaration

Funding Not applicable

Conflicts of interest/Competing interests Not applicable

Availability of data and material Not applicable

Code availability Not applicable

Ethics approval Not applicable

References

1. Giordano G, Blanchini F, Bruno R, Colaneri P, Di Filippo A, Di Matteo A, et al. Modelling the COVID-19 epidemic and implementation of population-wide interventions in Italy. *Nature Medicine*. 2020;26(6):855-60. Available from: <https://doi.org/10.1038/s41591-020-0883-7>.
2. Nikolopoulos K, Punia S, Schäfers A, Tsinopoulos C, Vasilakis C. Forecasting and planning during a pandemic: COVID-19 growth rates, supply chain disruptions, and governmental decisions. *Eur J Oper Res*. 2021 Apr;290(1):99-115.
3. Campillo-Funollet E, Van Yperen J, Allman P, Bell M, Beresford W, Clay J, et al. Predicting and forecasting the impact of local outbreaks of COVID-19: use of SEIR-D quantitative epidemiological modelling for healthcare demand and capacity. *Int J Epidemiol*. 2021 Aug;50(4):1103-13.
4. Ioannidis JPA, Cripps S, Tanner MA. Forecasting for COVID-19 has failed. *Int J Forecast*. 2020 Aug.
5. Lazebnik T, Shami L, Bunimovich-Mendrazitsky S. Spatio-Temporal influence of Non-Pharmaceutical interventions policies on pandemic dynamics and the economy: the case of COVID-19. *Economic Research-Ekonomska Istraživanja*. 2021;0(0):1-29. Available from: <https://doi.org/10.1080/1331677X.2021.1925573>.
6. Silva PCL, Batista PVC, Lima HS, Alves MA, Guimarães FG, Silva RCP. COVID-ABS: An agent-based model of COVID-19 epidemic to simulate health and economic effects of social distancing interventions. *Chaos Solitons Fractals*. 2020 Oct;139:110088.
7. Dietz K. The estimation of the basic reproduction number for infectious diseases. *Statistical Methods in Medical Research*. 1993;2(1):23-41. PMID: 8261248. Available from: <https://doi.org/10.1177/096228029300200103>.
8. Dublin LI, Lotka AJ. On the True Rate of Natural Increase. *Journal of the American Statistical Association*. 1925 2020/09/20/;20(151):305-39. Full publication date: Sep., 1925. Available from: <http://www.jstor.org/stable/2965517>.
9. Lotka AJ. The measure of net fertility. *Journal of the Washington Academy of Sciences*. 1925;15(21):469-72. Available from: <http://www.jstor.org/stable/24527482>.
10. Heesterbeek JAP, Dietz K. The concept of R_0 in epidemic theory. *Statistica Neerlandica* 50: 89-110. 1993 01.
11. Heesterbeek JAP. A Brief History of R_0 and a Recipe for its Calculation. *Acta Biotheoretica*. 2002 Sep;50(3):189-204. Available from: <https://doi.org/10.1023/A:1016599411804>.
12. Dietz K. Transmission and control of arbovirus diseases. In *Proceedings of the Society for Industrial and Applied Mathematics, Epidemiology*: Philadelphia. 1975:104-21.
13. Delamater PL, Street EJ, Leslie TF, Yang YT, Jacobsen KH. Complexity of the Basic Reproduction Number (\mathcal{R}_0). *Emerg Infect Dis*. 2019 Jan;25(1):1-4.
14. Zhang Y, You C, Cai Z, Sun J, Hu W, Zhou XH. Prediction of the COVID-19 outbreak in China based on a new stochastic dynamic model. *Scientific Reports*. 2020;10(1):21522. Available from: <https://doi.org/10.1038/s41598-020-76630-0>.
15. Podolski P, Nguyen HS. Cellular Automata in COVID-19 prediction. *Procedia Comput Sci*. 2021;192:3370-9.
16. Hoertel N, Blachier M, Blanco C, Olfson M, Massetti M, Rico MS, et al. A stochastic agent-based model of the SARS-CoV-2 epidemic in France. *Nature Medicine*. 2020;26(9):1417-21. Available from: <https://doi.org/10.1038/s41591-020-1001-6>.
17. Firth JA, Hellewell J, Klepac P, Kissler S, Jit M, Atkins KE, et al. Using a real-world network to model localized COVID-19 control strategies. *Nature Medicine*. 2020;26(10):1616-22. Available from: <https://doi.org/10.1038/s41591-020-1036-8>.
18. Maurya S, Singh S. Time Series Analysis of the COVID-19 Datasets. In: 2020 IEEE International Conference for Innovation in Technology (INOCON); 2020. p. 1-6.
19. Shaikh S, Gala J, Jain A, Advani S, Jaidhara S, Roja Edinburgh M. Analysis and Prediction of COVID-19 using Regression Models and Time Series Forecasting. In: 2021 11th International Conference on Cloud Computing, Data Science Engineering (Confluence); 2021. p. 989-95.
20. Zeroual A, Harrou F, Dairi A, Sun Y. Deep learning methods for forecasting COVID-19 time-Series data: A Comparative study. *Chaos Solitons & Fractals*. 2020 Nov;140:110121.

21. Cardoso BHF, Gonçalves S. Universal scaling law for human-to-human transmission diseases. *EPL (Europhysics Letters)*. 2021 mar;133(5):58001. Available from: <https://doi.org/10.1209/0295-5075/133/58001>.
22. Sy KTL, White LF, Nichols BE. Population density and basic reproductive number of COVID-19 across United States counties. *PLOS ONE*. 2021 04;16(4):1-11. Available from: <https://doi.org/10.1371/journal.pone.0249271>.
23. Derakhshan M, Ansarian HR, Ghomshei M. Temporal variations in COVID-19: an epidemiological discussion with a practical application. *J Int Med Res*. 2021 Aug;49(8):3000605211033208.
24. Cherednik I. Modeling the Waves of Covid-19. *Acta Biotheoretica*. 2021;70(1):8. Available from: <https://doi.org/10.1007/s10441-021-09428-w>.
25. Cacciapaglia G, Cot C, Sannino F. Multiwave pandemic dynamics explained: how to tame the next wave of infectious diseases. *Scientific Reports*. 2021;11(1):6638. Available from: <https://doi.org/10.1038/s41598-021-85875-2>.
26. Hethcote HW, Levin SA. Periodicity in Epidemiological Models. In: Levin SA, Hallam TG, Gross LJ, editors. *Applied Mathematical Ecology*. vol. 18 of *Biomathematics*. Berlin Heidelberg: Springer; 1989. p. 193-211.
27. Buonomo B, Chitnis N, d'Onofrio A. Seasonality in epidemic models: a literature review. *Ricerche di Matematica*. 2018;67(1):7-25. Available from: <https://doi.org/10.1007/s11587-017-0348-6>.
28. Ochab M, Manfredi P, Puzynski K, d'Onofrio A. Multiple epidemic waves as the outcome of stochastic SIR epidemics with behavioral responses: a hybrid modeling approach. *Nonlinear Dynamics*. 2022. Available from: <https://doi.org/10.1007/s11071-022-07317-6>.
29. Brand SPC, Ojal J, Aziza R, Were V, Okiro EA, Kombe IK, et al. COVID-19 transmission dynamics underlying epidemic waves in Kenya. *Science*. 2021 Nov;374(6570):989-94.
30. Tkachenko AV, Maslov S, Elbanna A, Wong GN, Weiner ZJ, Goldenfeld N. Time-dependent heterogeneity leads to transient suppression of the COVID-19 epidemic, not herd immunity. *Proc Natl Acad Sci U S A*. 2021 Apr;118(17).
31. Lauring AS, Tenforde MW, Chappell JD, Gaglani M, Ginde AA, McNeal T, et al. Clinical severity of, and effectiveness of mRNA vaccines against, covid-19 from omicron, delta, and alpha SARS-CoV-2 variants in the United States: prospective observational study. *BMJ*. 2022;376. Available from: <https://www.bmj.com/content/376/bmj-2021-069761>.
32. Saha S, Tanmoy AM, Tanni AA, Goswami S, Sium SMA, Saha S, et al. New waves, new variants, old inequity: a continuing COVID-19 crisis. *BMJ Global Health*. 2021;6(8). Available from: <https://gh.bmj.com/content/6/8/e007031>.
33. Callaway E. The coronavirus is mutating - does it matter? *Nature*. 2020 Sep;585(7824):174-7.
34. Arribas M, Aguirre J, Manrubia S, Lázaro E. Differences in adaptive dynamics determine the success of virus variants that propagate together. *Virus Evol*. 2018 Jan;4(1):vex043.
35. Kupferschmidt K. The pandemic virus is slowly mutating. But does it matter? *Science*. 2020;369(6501):238-9. Available from: <https://www.science.org/doi/abs/10.1126/science.369.6501.238>.
36. Boehm E, Kronig I, Neher RA, Eckerle I, Vetter P, Kaiser L. Novel SARS-CoV-2 variants: the pandemics within the pandemic. *Clinical Microbiology and Infection*. 2021;27(8):1109-17. Available from: <https://www.sciencedirect.com/science/article/pii/S1198743X21002627>.
37. Luna-Muschi A, Borges IC, de Faria E, Barboza AS, Maia FL, Leme MD, et al. Clinical features of COVID-19 by SARS-CoV-2 Gamma variant: A prospective cohort study of vaccinated and unvaccinated healthcare workers. *J Infect*. 2022 Feb;84(2):248-88.
38. Nyberg T, Ferguson NM, Nash SG, Webster HH, Flaxman S, Andrews N, et al. Comparative analysis of the risks of hospitalisation and death associated with SARS-CoV-2 omicron (B.1.1.529) and delta (B.1.617.2) variants in England: a cohort study. *The Lancet*. 2022;399(10332):1303-12. Available from: <https://www.sciencedirect.com/science/article/pii/S0140673622004627>.

39. Vargas-Herrera N, Araujo-Castillo RV, Mestanza O, Galarza M, Rojas-Serrano N, Solari-Zerpa L. SARS-CoV-2 Lambda and Gamma variants competition in Peru, a country with high seroprevalence. *Lancet Regional Health Americas*. 2022 02;6:100112-2. Available from: <https://pubmed.ncbi.nlm.nih.gov/34812432>.
40. Roberts M, Andreasen V, Lloyd A, Pellis L. Nine challenges for deterministic epidemic models. *Epidemics*. 2015 Mar;10:49-53.
41. Bessièrè P, Volmer R. From one to many: The within-host rise of viral variants. *PLOS Pathogens*. 2021 09;17(9):1-5. Available from: <https://doi.org/10.1371/journal.ppat.1009811>.
42. Korber B, Fischer WM, Gnanakaran S, Yoon H, Theiler J, Abfalterer W, et al. Tracking Changes in SARS-CoV-2 Spike: Evidence that D614G Increases Infectivity of the COVID-19 Virus [doi: 10.1016/j.cell.2020.06.043]. *Cell*. 2020 2022/07/02;182(4):812-27.e19. Available from: <https://doi.org/10.1016/j.cell.2020.06.043>.
43. Benjamin RL. The hybrid incidence susceptible-transmissible-removed model for pandemics; 2021. Pre-print ACTA Biotheoretica. Available from: <http://philsci-archive.pitt.edu/19821/>.
44. Kermack WO, McKendrick AG. Contributions to the mathematical theory of epidemics—I. 1927. *Bull Math Biol*. 1991;53(1-2):33-55.
45. Kermack WO, McKendrick AG. Contributions to the mathematical theory of epidemics—II. The problem of endemicity. 1932. *Bull Math Biol*. 1991;53(1-2):57-87.
46. Kermack WO, McKendrick AG. Contributions to the mathematical theory of epidemics—III. Further studies of the problem of endemicity. 1933. *Bull Math Biol*. 1991;53(1-2):89-118.
47. Hamer WH. The Milroy Lectures ON EPIDEMIC DISEASE IN ENGLAND—THE EVIDENCE OF VARIABILITY AND OF PERSISTENCY OF TYPE. *The Lancet*. 1906;167(4305):569-574. Originally published as Volume 1, Issue 4305. Available from: <http://www.sciencedirect.com/science/article/pii/S0140673601801872>.
48. Moore CA, Ruisch BC, Granados Samayoa JA, Boggs ST, Ladanyi JT, Fazio RH. Contracting COVID-19: a longitudinal investigation of the impact of beliefs and knowledge. *Scientific Reports*. 2021 Oct;11(1):20460. Available from: <https://doi.org/10.1038/s41598-021-99981-8>.
49. Varghese A, Kolamban S, Sherimon V, Lacap EM, Ahmed SS, Sreedhar JP, et al. SEAMHCRD deterministic compartmental model based on clinical stages of infection for COVID-19 pandemic in Sultanate of Oman. *Scientific Reports*. 2021;11(1):11984. Available from: <https://doi.org/10.1038/s41598-021-91114-5>.
50. Lyra W, do Nascimento JD Jr, Belkhiria J, de Almeida L, Chrispim PPM, de Andrade I. COVID-19 pandemics modeling with modified determinist SEIR, social distancing, and age stratification. The effect of vertical confinement and release in Brazil. *PLOS ONE*. 2020 09;15(9):1-17. Available from: <https://doi.org/10.1371/journal.pone.0237627>.
51. Rădulescu A, Williams C, Cavanagh K. Management strategies in a SEIR-type model of COVID 19 community spread. *Scientific Reports*. 2020;10(1):21256. Available from: <https://doi.org/10.1038/s41598-020-77628-4>.
52. Ram V, Schaposnik LP. A modified age-structured SIR model for COVID-19 type viruses. *Scientific Reports*. 2021;11(1):15194. Available from: <https://doi.org/10.1038/s41598-021-94609-3>.
53. Balabdaoui F, Mohr D. Age-stratified discrete compartment model of the COVID-19 epidemic with application to Switzerland. *Scientific Reports*. 2020;10(1):21306. Available from: <https://doi.org/10.1038/s41598-020-77420-4>.
54. Jewell NP, Lewnard JA, Jewell BL. Predictive Mathematical Models of the COVID-19 Pandemic: Underlying Principles and Value of Projections. *JAMA*. 2020 May;323(19):1893-4.
55. Holmdahl I, Buckee C. Wrong but Useful — What COVID-19 Epidemiologic Models Can and Cannot Tell Us. *New England Journal of Medicine*. 2020;383(4):303-5. Available from: <https://doi.org/10.1056/NEJMp2016822>.
56. Dell’Anna L. Solvable delay model for epidemic spreading: the case of COVID-19 in Italy. *Scientific Reports*. 2020;10(1):15763. Available from: <https://doi.org/10.1038/s41598-020-72529-y>.

57. Devipriya R, Dhamodharavadhani s, Selvi S. SEIR Model for COVID-19 Epidemic Using Delay Differential Equation. *Journal of Physics: Conference Series*. 2021 02;1767:012005.
58. Feng S, Feng Z, Ling C, Chang C, Feng Z. Prediction of the COVID-19 epidemic trends based on SEIR and AI models. *PLOS ONE*. 2021 01;16(1):1-15. Available from: <https://doi.org/10.1371/journal.pone.0245101>.
59. Carcione JM, Santos JE, Bagaini C, Ba J. A Simulation of a COVID-19 Epidemic Based on a Deterministic SEIR Model. *Frontiers in Public Health*. 2020;8:230. Available from: <https://www.frontiersin.org/article/10.3389/fpubh.2020.00230>.
60. Khedher Nb, Kolsi L, Alsaif H. A multi-stage SEIR model to predict the potential of a new COVID-19 wave in KSA after lifting all travel restrictions. *Alexandria Engineering Journal*. 2021 08;60(4):3965-74. Available from: <https://www.ncbi.nlm.nih.gov/pmc/articles/PMC7927593/>.
61. Walsh KA, Spillane S, Comber L, Cardwell K, Harrington P, Connell J, et al. The duration of infectiousness of individuals infected with SARS-CoV-2. *J Infect*. 2020 Dec;81(6):847-56.
62. Lythgoe KA, Fraser C. New insights into the evolutionary rate of HIV-1 at the within-host and epidemiological levels. *Proceedings of the Royal Society B: Biological Sciences*. 2012;279(1741):3367-75. Available from: <https://royalsocietypublishing.org/doi/abs/10.1098/rspb.2012.0595>.
63. Wang HY, Yamamoto N. Using a partial differential equation with Google Mobility data to predict COVID-19 in Arizona. *Math Biosci Eng*. 2020 Jul;17(5):4891-904.
64. Viguerie A, Lorenzo G, Auricchio F, Baroli D, Hughes TJR, Patton A, et al. Simulating the spread of COVID-19 via a spatially-resolved susceptible-exposed-infected-recovered-deceased (SEIRD) model with heterogeneous diffusion. *Appl Math Lett*. 2021 Jan;111:106617.
65. Chalub FACC, Souza MO. The SIR epidemic model from a PDE point of view. *Mathematical and Computer Modelling*. 2011;53(7):1568-74. *Mathematical Methods and Modelling of Biophysical Phenomena*. Available from: <https://www.sciencedirect.com/science/article/pii/S0895717710002906>.
66. Lefevre C, Picard P, Simon M, Utev S. A chain binomial epidemic with asymptomatics motivated by COVID-19 modelling. *Journal of mathematical biology*. 2021 11;83(5):54-4. Available from: <https://pubmed.ncbi.nlm.nih.gov/34725739>.
67. Hellewell J, Abbott S, Gimma A, Bosse NI, Jarvis CI, Russell TW, et al. Feasibility of controlling COVID-19 outbreaks by isolation of cases and contacts. *The Lancet Global health*. 2020 04;8(4):e488-96. Available from: <https://pubmed.ncbi.nlm.nih.gov/32119825>.
68. Levesque J, Maybury DW, Shaw RHAD. A model of COVID-19 propagation based on a gamma subordinated negative binomial branching process. *Journal of theoretical biology*. 2021 03;512:110536-6. Available from: <https://pubmed.ncbi.nlm.nih.gov/33186594>.
69. Niu R, Chan YC, Wong EWM, van Wyk MA, Chen G. A stochastic SEIHR model for COVID-19 data fluctuations. *Nonlinear dynamics*. 2021 07:1-13. Available from: <https://pubmed.ncbi.nlm.nih.gov/34248280>.
70. Zhang Z, Zeb A, Hussain S, Alzahrani E. Dynamics of COVID-19 mathematical model with stochastic perturbation. *Advances in difference equations*. 2020;2020(1):451-1. Available from: <https://pubmed.ncbi.nlm.nih.gov/32874186>.
71. Dordevic J, Papic I, Suvak N. A two diffusion stochastic model for the spread of the new corona virus SARS-CoV-2. *Chaos, solitons, and fractals*. 2021 07;148:110991-1. Available from: <https://pubmed.ncbi.nlm.nih.gov/33967408>.
72. Allen LJS, Burgin AM. Comparison of deterministic and stochastic SIS and SIR models in discrete time. *Mathematical Biosciences*. 2000;163(1):1-33. Available from: <https://www.sciencedirect.com/science/article/pii/S0025556499000474>.
73. Osthus D, Hickmann KS, Caragea PC, Higdon D, Del Valle SY. Forecasting seasonal influenza with a state-space SIR model. *Ann Appl Stat*. 2017 Mar;11(1):202-24.
74. Newman MEJ. Spread of epidemic disease on networks. *Phys Rev E*. 2002 Jul;66:016128. Available from: <https://link.aps.org/doi/10.1103/PhysRevE.66.016128>.

75. Moreno Y, Pastor-Satorras R, Vespignani A. Epidemic outbreaks in complex heterogeneous networks. *The European Physical Journal B - Condensed Matter and Complex Systems*. 2002;26(4):521-9. Available from: <https://doi.org/10.1140/epjb/e20020122>.
76. Schimit PHT, Pereira FH. Disease spreading in complex networks: A numerical study with Principal Component Analysis. *Expert Syst Appl*. 2018 May;97:41-50.
77. Pastor-Satorras R, Castellano C, Van Mieghem P, Vespignani A. Epidemic processes in complex networks. *Rev Mod Phys*. 2015 Aug;87:925-79. Available from: <https://link.aps.org/doi/10.1103/RevModPhys.87.925>.
78. Rorres C, Romano M, Miller JA, Mossey JM, Grubestic TH, Zellner DE, et al. Contact tracing for the control of infectious disease epidemics: Chronic Wasting Disease in deer farms. *Epidemics*. 2018;23:71-5. Available from: <https://www.sciencedirect.com/science/article/pii/S1755436517301883>.
79. Pavlopoulos GA, Secrier M, Moschopoulos CN, Soldatos TG, Kossida S, Aerts J, et al. Using graph theory to analyze biological networks. *BioData mining*. 2011 04;4:10-0. Available from: <https://pubmed.ncbi.nlm.nih.gov/21527005>.
80. Read JM, Eames KTD, Edmunds WJ. Dynamic social networks and the implications for the spread of infectious disease. *J R Soc Interface*. 2008 Sep;5(26):1001-7.
81. Jo W, Chang D, You M, Ghim GH. A social network analysis of the spread of COVID-19 in South Korea and policy implications. *Scientific Reports*. 2021;11(1):8581. Available from: <https://doi.org/10.1038/s41598-021-87837-0>.
82. Block P, Hoffman M, Raabe IJ, Dowd JB, Rahal C, Kashyap R, et al. Social network-based distancing strategies to flatten the COVID-19 curve in a post-lockdown world. *Nature Human Behaviour*. 2020;4(6):588-96. Available from: <https://doi.org/10.1038/s41562-020-0898-6>.
83. Del Valle SY, Hyman JM, Hethcote HW, Eubank SG. Mixing patterns between age groups in social networks. *Social Networks*. 2007;29(4):539-54. Available from: <https://www.sciencedirect.com/science/article/pii/S0378873307000330>.
84. Silva CJ, Cantin G, Cruz C, Fonseca-Pinto R, Passadouro R, Soares Dos Santos E, et al. Complex network model for COVID-19: Human behavior, pseudo-periodic solutions and multiple epidemic waves. *J Math Anal Appl*. 2021 Mar:125171.
85. Kucharski R, Cats O, Sienkiewicz J. Modelling virus spreading in ride-pooling networks. *Scientific Reports*. 2021;11(1):7201. Available from: <https://doi.org/10.1038/s41598-021-86704-2>.
86. Lazebnik T, Bunimovich-Mendrazitsky S, Shami L. Pandemic management by a spatio-temporal mathematical model. *International Journal of Nonlinear Sciences and Numerical Simulation*. 2021:000010151520210063. Available from: <https://doi.org/10.1515/ijnsns-2021-0063>.
87. Thurner S, Klimek P, Hanel R. A network-based explanation of why most COVID-19 infection curves are linear. *Proceedings of the National Academy of Sciences*. 2020;117(37):22684-9. Available from: <https://www.pnas.org/content/117/37/22684>.
88. Fall A, Fortin MJ, Manseau M, O'Brien D. Spatial Graphs: Principles and Applications for Habitat Connectivity. *Ecosystems*. 2007;10(3):448-61. Available from: <https://doi.org/10.1007/s10021-007-9038-7>.
89. Kerr CC, Stuart RM, Mistry D, Abeyesuriya RG, Rosenfeld K, Hart GR, et al. Covasim: An agent-based model of COVID-19 dynamics and interventions. *PLoS Comput Biol*. 2021 Jul;17(7):e1009149.
90. Najmi A, Nazari S, Safarighouzhdi F, Miller EJ, MacIntyre R, Rashidi TH. Easing or tightening control strategies: determination of COVID-19 parameters for an agent-based model. *Transportation*. 2021. Available from: <https://doi.org/10.1007/s11116-021-10210-7>.
91. Medrek M, Pastuszak Z. Numerical simulation of the novel coronavirus spreading. *Expert Systems with Applications*. 2021;166:114109. Available from: <https://www.sciencedirect.com/science/article/pii/S0957417420308605>.
92. Zhou Y, Wang L, Zhang L, Shi L, Yang K, He J, et al. A Spatiotemporal Epidemiological Prediction Model to Inform County-Level COVID-19 Risk in the United States. *Harvard Data Science Review*. 2020 8. <https://hdsr.mitpress.mit.edu/pub/qqg19a0r>. Available from: <https://hdsr.mitpress.mit.edu/pub/qqg19a0r>.

93. Schimit PHT. A model based on cellular automata to estimate the social isolation impact on COVID-19 spreading in Brazil. *Comput Methods Programs Biomed.* 2021 Mar;200:105832.
94. Almeida Simoes J. An agent-based approach to spatial epidemics through GIS. University of London; 2007. Available from: <http://ethos.bl.uk/ProcessSearch.do?query=444185>.
95. Aguilar W, Santamaría-Bonfil G, Froese T, Gershenson C. The Past, Present, and Future of Artificial Life. *Frontiers in Robotics and AI.* 2014;1:8. Available from: <https://www.frontiersin.org/article/10.3389/frobt.2014.00008>.
96. Bonabeau E. Agent-based modeling: Methods and techniques for simulating human systems. *Proceedings of the National Academy of Sciences.* 2002;99(suppl 3):7280-7. Available from: https://www.pnas.org/content/99/suppl_3/7280.
97. Jin Z, Liu QX. A cellular automata model of epidemics of a heterogeneous susceptibility. *Chinese Physics.* 2006 05;15:1248.
98. Schneckenreither G, Popper N, Zauner G, Breitenecker F. Modelling SIR-type epidemics by ODEs, PDEs, difference equations and cellular automata – A comparative study. *Simulation Modelling Practice and Theory.* 2008;16(8):1014-23. *EUROSIM 2007.* Available from: <https://www.sciencedirect.com/science/article/pii/S1569190X08001160>.
99. Boccara N, Cheong K. Automata network SIR models for the spread of infectious diseases in populations of moving individuals. *Journal of Physics A: Mathematical and General.* 1992 may;25(9):2447-61. Available from: <https://doi.org/10.1088/0305-4470/25/9/018>.
100. Guo Z, Shi B, Wang N. Lattice BGK Model for Incompressible Navier–Stokes Equation. *Journal of Computational Physics.* 2000;165(1):288-306. Available from: <https://www.sciencedirect.com/science/article/pii/S0021999100966166>.
101. Montgomery D, Jennings C, Kulahci M. *Introduction to Time Series Analysis and Forecasting.* 2nd ed. Hoboken, New Jersey: Wiley; 2015.
102. Holloway JL. Smoothing and Filtering of Time Series and Space Fields. In: Landsberg HE, Van Mieghem J, editors. *Advances in Geophysics.* vol. 4. New York: Academic Press; 1958. p. 351-89. Available from: <https://www.sciencedirect.com/science/article/pii/S0065268708604872>.
103. Takefuji Y. Fourier analysis using the number of COVID-19 daily deaths in the US. *Epidemiology and Infection.* 2021;149:e64.
104. Kuzmenko OV, Smiiianov VA, Rudenko LA, Kashcha MO, Vasilyeva TA, Kolomiets SV, et al. IMPACT OF VACCINATION ON THE COVID-19 PANDEMIC: BIBLIOMETRIC ANALYSIS AND CROSS COUNTRY FORECASTING BY FOURIER SERIES. *Wiad Lek.* 2021;74(10 pt 1):2359-67.
105. Kashcha M, Palienko M, Marchenko R. Forecast of COVID-19 progress considering the seasonal fluctuations. *Health Economics and Management Review.* 2021;2:71-82. Available from: <http://doi.org/10.21272/hem.2021.2-07>.
106. Wang X, Washington D, Weber GF. Complex systems analysis informs on the spread of COVID-19. *Epidemiologic Methods.* 2021;10(s1):20210019. Available from: <https://doi.org/10.1515/em-2021-0019>.
107. Eubank RL. *A Kalman Filter Primer.* Boca Raton, FL: Chapman & Hall/CRC; 2006.
108. Bisgaard S, Kulahci M. *Time Series Analysis and Forecasting by Example.* 1st ed. Hoboken, NJ: Wiley; 2011.
109. Box GEP, Jenkins GM, Reinsel GC, Ljung GM. *TIME SERIES ANALYSIS Forecasting and Control.* 5th ed. Hoboken, New Jersey: Wiley; 2016.
110. Papastefanopoulos V, Linardatos P, Kotsiantis S. COVID-19: A Comparison of Time Series Methods to Forecast Percentage of Active Cases per Population. *Applied Sciences.* 2020;10(11). Available from: <https://www.mdpi.com/2076-3417/10/11/3880>.
111. Mills TC. *Applied Time Series Analysis.* 1st ed. Mills TC, editor. New York: Academic Press; 2019.
112. Liao Z, Lan P, Liao Z, Zhang Y, Liu S. TW-SIR: time-window based SIR for COVID-19 forecasts. *Scientific Reports.* 2020;10(1):22454. Available from: <https://doi.org/10.1038/s41598-020-80007-8>.

113. Maleki M, Mahmoudi MR, Heydari MH, Pho KH. Modeling and forecasting the spread and death rate of coronavirus (COVID-19) in the world using time series models. *Chaos, Solitons & Fractals*. 2020;140:110151. Available from: <https://www.sciencedirect.com/science/article/pii/S0960077920305476>.
114. Rath S, Tripathy A, Tripathy AR. Prediction of new active cases of coronavirus disease (COVID-19) pandemic using multiple linear regression model. *Diabetes & Metabolic Syndrome: Clinical Research & Reviews*. 2020;14(5):1467-74. Available from: <https://www.sciencedirect.com/science/article/pii/S1871402120302939>.
115. Tan CV, Singh S, Lai CH, Zamri ASSM, Dass SC, Aris TB, et al. Forecasting COVID-19 Case Trends Using SARIMA Models during the Third Wave of COVID-19 in Malaysia. *International Journal of Environmental Research and Public Health*. 2022;19(3). Available from: <https://www.mdpi.com/1660-4601/19/3/1504>.
116. Zeroual A, Harrou F, Dairi A, Sun Y. Deep learning methods for forecasting COVID-19 time-Series data: A Comparative study. *Chaos, Solitons & Fractals*. 2020;140:110121. Available from: <https://www.sciencedirect.com/science/article/pii/S096007792030518X>.
117. Wiczorek M, Silka J, Woźniak M. Neural network powered COVID-19 spread forecasting model. *Chaos, Solitons & Fractals*. 2020;140:110203. Available from: <https://www.sciencedirect.com/science/article/pii/S0960077920305993>.
118. Hssayeni MD, Chala A, Dev R, Xu L, Shaw J, Furht B, et al. The forecast of COVID-19 spread risk at the county level. *Journal of big data*. 2021;8(1):99-9. Available from: <https://pubmed.ncbi.nlm.nih.gov/34249603>.
119. Commandeur JFF, Koopman SJ. An introduction to State-Space time series analysis. 1st ed. *Practical Econometrics*. Oxford, UK: Oxford University Press; 2007.
120. Watson O, Alhaffer M, Mehchy Z, Whittaker C, et al. Report 31: Estimating the burden of COVID-19 in Damascus, Syria: an analysis of novel data sources to infer mortality under-ascertainment; 2020. <https://doi.org/10.25561/82443>.
121. Proverbio D, Kemp F, Magni S, Ogorzaly L, Cauchie HM, Gonçalves J, et al. Model-based assessment of COVID-19 epidemic dynamics by wastewater analysis. *Science of The Total Environment*. 2022:154235. Available from: <https://www.sciencedirect.com/science/article/pii/S0048969722013274>.
122. Woolf SH, Chapman DA, Sabo RT, Weinberger DM, Hill L, Taylor DDH. Excess Deaths From COVID-19 and Other Causes, March-July 2020. *JAMA*. 2020 10;324(15):1562-4. Available from: <https://pubmed.ncbi.nlm.nih.gov/33044483>.
123. Achilleos S, Quattrocchi A, Gabel J, Heraclides A, Kolokotroni O, Constantinou C, et al. Excess all-cause mortality and COVID-19-related mortality: a temporal analysis in 22 countries, from January until August 2020. *International journal of epidemiology*. 2022 02;51(1):35-53. Available from: <https://pubmed.ncbi.nlm.nih.gov/34282450>.
124. Lee D, Heo K, Seo Y. COVID-19 in South Korea: Lessons for developing countries. *World Development*. 2020;135:105057. Available from: <https://www.sciencedirect.com/science/article/pii/S0305750X20301832>.
125. Lindner AK, Sarma N, Rust LM, Hellmund T, Krasovski-Nikiforovs S, Wintel M, et al. Monitoring for COVID-19 by universal testing in a homeless shelter in Germany: a prospective feasibility cohort study. *BMC infectious diseases*. 2021 12;21(1):1241-1. Available from: <https://pubmed.ncbi.nlm.nih.gov/34895157>.
126. O'Shea T, Mbuagbaw L, Mokashi V, Bulir D, Gilchrist J, Smieja N, et al. Comparison of four COVID-19 screening strategies to facilitate early case identification within the homeless shelter population: A structured summary of a study protocol for a randomised controlled trial. *Trials*. 2020;21(1):941. Available from: <https://doi.org/10.1186/s13063-020-04890-2>.
127. Silva PJS, Pereira T, Sagastizábal C, Nonato L, Cordova MM, Struchiner CJ. Smart testing and critical care bed sharing for COVID-19 control. *PLOS ONE*. 2021 10;16(10):1-17. Available from: <https://doi.org/10.1371/journal.pone.0257235>.
128. Arons MM, Hatfield KM, Reddy SC, Kimball A, James A, Jacobs JR, et al. Presymptomatic SARS-CoV-2 Infections and Transmission in a Skilled Nursing Facility. *New England Journal of Medicine*. 2020;382(22):2081-90. Available from: <https://doi.org/10.1056/NEJMoa2008457>.

129. Nishiura H, Kobayashi T, Yang Y, Hayashi K, Miyama T, Kinoshita R, et al. The Rate of Underascertainment of Novel Coronavirus (2019-nCoV) Infection: Estimation Using Japanese Passengers Data on Evacuation Flights. *Journal of Clinical Medicine*. 2020;9(2). Available from: <https://www.mdpi.com/2077-0383/9/2/419>.
130. Mizumoto K, Kagaya K, Zarebski A, Chowell G. Estimating the asymptomatic proportion of coronavirus disease 2019 (COVID-19) cases on board the Diamond Princess cruise ship, Yokohama, Japan, 2020. *Euro Surveill*. 2020 Mar;25(10).
131. Ing AJ, Cocks C, Green JP. COVID-19: in the footsteps of Ernest Shackleton. *Thorax*. 2020 08;75(8):693-4. Available from: <https://pubmed.ncbi.nlm.nih.gov/32461231>.
132. Yoo KJ, Kwon S, Choi Y, Bishai DM. Systematic assessment of South Korea's capabilities to control COVID-19. *Health Policy*. 2021;125(5):568-76. Available from: <https://www.sciencedirect.com/science/article/pii/S0168851021000543>.
133. Majeed A, Seo Y, Heo K, Lee D. Can the UK emulate the South Korean approach to COVID-19? *BMJ*. 2020;369. Available from: <https://www.bmj.com/content/369/bmj.m2084>.
134. Arroyo-Marioli F, Bullano F, Kucinskas S, Rondón-Moreno C. Tracking R of COVID-19: A new real-time estimation using the Kalman filter. *PLOS ONE*. 2021 01;16(1):1-16. Available from: <https://doi.org/10.1371/journal.pone.0244474>.
135. Song J, Xie H, Gao B, Zhong Y, Gu C, Choi KS. Maximum likelihood-based extended Kalman filter for COVID-19 prediction. *Chaos, solitons, and fractals*. 2021 05;146:110922-2. Available from: <https://pubmed.ncbi.nlm.nih.gov/33824550>.
136. Koyama S, Horie T, Shinomoto S. Estimating the time-varying reproduction number of COVID-19 with a state-space method. *PLOS Computational Biology*. 2021 01;17(1):1-18. Available from: <https://doi.org/10.1371/journal.pcbi.1008679>.
137. Aslam M. Using the Kalman filter with ARIMA for the COVID-19 pandemic dataset of Pakistan. *Data in Brief*. 2020;31:105854. Available from: <https://www.sciencedirect.com/science/article/pii/S2352340920307484>.
138. Assimakis N, Ktena A, Manasis C, Mele E, Kunicina N, Zabasta A, et al. Using the time varying Kalman filter for prediction of COVID-19 cases in Latvia and Greece. In: 2020 IEEE 61th International Scientific Conference on Power and Electrical Engineering of Riga Technical University (RTUCON); 2020. p. 1-7.
139. Singh KK, Kumar S, Dixit P, Bajpai MK. Kalman filter based short term prediction model for COVID-19 spread. *Applied Intelligence*. 2021;51(5):2714-26. Available from: <https://doi.org/10.1007/s10489-020-01948-1>.
140. Flaxman S, Mishra S, Gandy A, et al. Report 13: Estimating the number of infections and the impact of non-pharmaceutical interventions on COVID-19 in 11 European countries; 2020. <https://doi.org/10.25561/77731>.
141. Hopkins University of Medicine Coronavirus Resource Center J. NEW COVID-19 CASES WORLDWIDE;. Available from: <https://coronavirus.jhu.edu/data/new-cases> [cited 29 May 2021].
142. Hu H, Nigmatulina K, Eckhoff P. The scaling of contact rates with population density for the infectious disease models. *Mathematical Biosciences*. 2013;244(2):125-34. Available from: <https://www.sciencedirect.com/science/article/pii/S0025556413001235>.
143. Heesterbeek JAP. 5. In: K C, B B, editors. *The law of mass-action in epidemiology: A historical perspective*. Burlington, MA: Academic Press; 2005. p. 81-105.
144. Ferner RE, Aronson JK. Cato Guldberg and Peter Waage, the history of the Law of Mass Action, and its relevance to clinical pharmacology. *Br J Clin Pharmacol*. 2016 Jan;81(1):52-5.
145. Adleman L, Gopalkrishnan M, Huang Md, Moisset P, Reishus D. 1. In: *On the Mathematics of the Law of Mass Action*. Dordrecht: Springer; 2008. p. 3-46.
146. Brauer F, Castillo-Chávez C, Feng Z. *Mathematical Models in Epidemiology*. Netherlands: Springer; 2019.
147. Patterson O. Making Sense of Culture. *Annual Review of Sociology*. 2014;40(1):1-30. Available from: <https://doi.org/10.1146/annurev-soc-071913-043123>.
148. Suvilehto JT, Nummenmaa L, Harada T, Dunbar RIM, Hari R, Turner R, et al. Cross-cultural similarity in relationship-specific social touching. *Proceedings Biological sciences*. 2019 04;286(1901):20190467-7. Available from: <https://pubmed.ncbi.nlm.nih.gov/31014213>.

149. Juliette H, Unwin T, Mishra S, Bradley V, *et al.* Report 23: State-level tracking of COVID-19 in the United States; 2020. <https://doi.org/10.25561/79231>.
150. Population sizes and densities for Countries and States; 2021. Available from: <https://worldpopulationreview.com> [cited 01/02/2021].
151. Davies NG, Klepac P, Liu Y, Prem K, Jit M, Pearson CAB, *et al.* Age-dependent effects in the transmission and control of COVID-19 epidemics. *Nature Medicine*. 2020;26(8):1205-11. Available from: <https://doi.org/10.1038/s41591-020-0962-9>.
152. Guo W, Li M, Dong Y, Zhou H, Zhang Z, Tian C, *et al.* Diabetes is a risk factor for the progression and prognosis of COVID-19. *Diabetes/metabolism research and reviews*. 2020 03:e3319-9. Available from: <https://pubmed.ncbi.nlm.nih.gov/32233013>.
153. Singh AK, Gupta R, Ghosh A, Misra A. Diabetes in COVID-19: Prevalence, pathophysiology, prognosis and practical considerations. *Diabetes & metabolic syndrome*. 2020 Jul-Aug;14(4):303-10. Available from: <https://pubmed.ncbi.nlm.nih.gov/32298981>.
154. Brooks J. The sad and tragic life of Typhoid Mary. *CMAJ : Canadian Medical Association journal = journal de l'Association medicale canadienne*. 1996 03;154(6):915-6. Available from: <https://pubmed.ncbi.nlm.nih.gov/8634973>.
155. Guest C. 6.6. In: *Oxford Handbook of public health practice*. 3rd ed. Oxford, UK: Oxford University Press; 2013. p. 474.
156. Chen H, Shi L, Zhang Y, Wang X, Jiao J, Yang M, *et al.* Response to the COVID-19 Pandemic: Comparison of Strategies in Six Countries. *Frontiers in public health*. 2021 09;9:708496-6. Available from: <https://pubmed.ncbi.nlm.nih.gov/34660510>.
157. Walker PGT, Whittaker C, Watson OJ, Baguelin M, Winskill P, Hamlet A, *et al.* The impact of COVID-19 and strategies for mitigation and suppression in low- and middle-income countries. *Science*. 2020;369(6502):413-22. Available from: <https://www.science.org/doi/abs/10.1126/science.abc0035>.
158. Spinney L. How elimination versus suppression became Covid's cold war;. Available from: <https://www.theguardian.com/commentisfree/2021/mar/03/covid-19-elimination-versus-suppression> [cited 13/03/2022].
159. Ludvigsson JF. The first eight months of Sweden's COVID-19 strategy and the key actions and actors that were involved. *Acta Paediatrica*. 2020;109(12):2459-71. Available from: <https://onlinelibrary.wiley.com/doi/abs/10.1111/apa.15582>.
160. Paterlini M. What now for Sweden and COVID-19? *BMJ*. 2021;375. Available from: <https://www.bmj.com/content/375/bmj.n3081>.
161. Woodward A. Yes, the coronavirus mutates. But those tiny changes haven't affected how dangerous it is — instead, they help scientists track its spread;. Available from: <https://www.businessinsider.com/coronavirus-mutations-strains-scientists-track-genetics-2020-4?IR=T> [cited 13/03/2022].
162. Krumholz HM, Ross JS, Presler AH, Egilman DS. What have we learnt from Vioxx? *BMJ (Clinical research ed)*. 2007 01;334(7585):120-3. Available from: <https://pubmed.ncbi.nlm.nih.gov/17235089>.
163. Schwartz JL. The first rotavirus vaccine and the politics of acceptable risk. *The Milbank quarterly*. 2012 06;90(2):278-310. Available from: <https://pubmed.ncbi.nlm.nih.gov/22709389>.
164. Gagne J. Popular heartburn drug ranitidine recalled: What you need to know and do;. Available from: <https://www.health.harvard.edu/blog/popular-heartburn-drug-ranitidine-recalled-what-you-need-to-know-and-do-2019092817911> [cited 13/03/2022].
165. Van Egeren D, Novokhodko A, Stoddard M, Tran U, Zetter B, Rogers M, *et al.* Risk of rapid evolutionary escape from biomedical interventions targeting SARS-CoV-2 spike protein. *PLOS ONE*. 2021 04;16(4):1-17. Available from: <https://doi.org/10.1371/journal.pone.0250780>.
166. Barrett C, Koyama A, Alvarez P, *et al.* Risk for Newly Diagnosed Diabetes >30 Days After SARS-CoV MMWR Morb Mortal Wkly Rep-2 Infection Among Persons Aged <18 Years — United States, March 1, 2020–June 28, 2021. *MMWR Morb Mortal Wkly Rep*. 2022;71:59-65.

167. Evans S. Australia's PM battles for his political survival amid fallout over the Delta outbreak;. Available from: <https://www.independent.co.uk/news/world/australasia/australia-pm-scott-morrison-covid-lockdown-b1892025.html> [cited 13/03/2022].
168. Roy CM, Bukuluki P, Casey SE, Jagun MO, John NA, Mabhena N, et al. Impact of COVID-19 on Gender-Based Violence Prevention and Response Services in Kenya, Uganda, Nigeria, and South Africa: A Cross-Sectional Survey. *Frontiers in global women's health*. 2022 01;2:780771-1. Available from: <https://pubmed.ncbi.nlm.nih.gov/35156086>.
169. Malone C. 'Zero COVID' Hong Kong grapples with vegetable shortages; 2022. Available from: <https://www.aljazeera.com/economy/2022/2/8/zero-covid-hong-kong-grapples-with-vegetable-shortages> [cited 13/03/2022].
170. Quicktaks B. Why China Is Sticking With Its 'Covid Zero' Strategy;. Available from: <https://www.bloomberg.com/news/articles/2022-02-10/why-china-is-sticking-with-its-covid-zero-strategy-quicktake> [cited 13/03/2022].
171. Jalongo MR. The Effects of COVID-19 on Early Childhood Education and Care: Research and Resources for Children, Families, Teachers, and Teacher Educators. *Early childhood education journal*. 2021 05:1-12. Available from: <https://pubmed.ncbi.nlm.nih.gov/34054286>.
172. Rodriguez-Morales AJ, Cardona-Ospina JA, Gutiérrez-Ocampo E, Villamizar-Peña R, Holguin-Rivera Y, Escalera-Antezana JP, et al. Clinical, laboratory and imaging features of COVID-19: A systematic review and meta-analysis. *Travel Medicine and Infectious Disease*. 2020;34:101623. Available from: <https://www.sciencedirect.com/science/article/pii/S1477893920300910>.
173. Pormohammad A, Ghorbani S, Baradaran B, Khatami A, J Turner R, Mansournia MA, et al. Clinical characteristics, laboratory findings, radiographic signs and outcomes of 61,742 patients with confirmed COVID-19 infection: A systematic review and meta-analysis. *Microbial Pathogenesis*. 2020;147:104390. Available from: <https://www.sciencedirect.com/science/article/pii/S0882401020307567>.
174. Ghosh N, Nandi S, Saha I. A review on evolution of emerging SARS-CoV-2 variants based on spike glycoprotein. *International immunopharmacology*. 2022 04;105:108565-5. Available from: <https://pubmed.ncbi.nlm.nih.gov/35123183>.
175. Cosar B, Karagulleoglu ZY, Unal S, Ince AT, Uncuoglu DB, Tuncer G, et al. SARS-CoV-2 Mutations and their Viral Variants. *Cytokine & growth factor reviews*. 2022 02;63:10-22. Available from: <https://pubmed.ncbi.nlm.nih.gov/34580015>.
176. Harvey WT, Carabelli AM, Jackson B, Gupta RK, Thomson EC, Harrison EM, et al. SARS-CoV-2 variants, spike mutations and immune escape. *Nature Reviews Microbiology*. 2021;19(7):409-24. Available from: <https://doi.org/10.1038/s41579-021-00573-0>.
177. Yuki K, Fujiogi M, Koutsogiannaki S. COVID-19 pathophysiology: A review. *Clinical immunology (Orlando, Fla)*. 2020 06;215:108427-7. Available from: <https://pubmed.ncbi.nlm.nih.gov/32325252>.
178. Galanopoulos M, Gkeros F, Doukatas A, Karianakis G, Pontas C, Tsoukalas N, et al. COVID-19 pandemic: Pathophysiology and manifestations from the gastrointestinal tract. *World journal of gastroenterology*. 2020 08;26(31):4579-88. Available from: <https://pubmed.ncbi.nlm.nih.gov/32884218>.
179. Wang D, Hu B, Hu C, Zhu F, Liu X, Zhang J, et al. Clinical Characteristics of 138 Hospitalized Patients With 2019 Novel Coronavirus-Infected Pneumonia in Wuhan, China. *JAMA*. 2020 Mar;323(11):1061-9.
180. Girona-Alarcon M, Bobillo-Perez S, Sole-Ribalta A, Hernandez L, Guitart C, Suarez R, et al. The different manifestations of COVID-19 in adults and children: a cohort study in an intensive care unit. *BMC Infectious Diseases*. 2021;21(1):87. Available from: <https://doi.org/10.1186/s12879-021-05786-5>.
181. Wiersinga WJ, Rhodes A, Cheng AC, Peacock SJ, Prescott HC. Pathophysiology, Transmission, Diagnosis, and Treatment of Coronavirus Disease 2019 (COVID-19): A Review. *JAMA*. 2020 08;324(8):782-93. Available from: <https://doi.org/10.1001/jama.2020.12839>.

182. Bienvenu LA, Noonan J, Wang X, Peter K. Higher mortality of COVID-19 in males: sex differences in immune response and cardiovascular comorbidities. *Cardiovascular research*. 2020 12;116(14):2197-206. Available from: <https://pubmed.ncbi.nlm.nih.gov/33063089>.
183. Ramesh S, Govindarajulu M, Parise RS, Neel L, Shankar T, Patel S, et al. Emerging SARS-CoV-2 Variants: A Review of Its Mutations, Its Implications and Vaccine Efficacy. *Vaccines*. 2021 10;9(10):1195. Available from: <https://pubmed.ncbi.nlm.nih.gov/34696303>.
184. Awadasseid A, Wu Y, Tanaka Y, Zhang W. SARS-CoV-2 variants evolved during the early stage of the pandemic and effects of mutations on adaptation in Wuhan populations. *Int J Biol Sci*. 2021;17:97-106. Available from: <https://www.ijbs.com/v17p0097.htm>.
185. SeyedAlinaghi S, Mirzapour P, Dadras O, Pashaei Z, Karimi A, MohsseniPour M, et al. Characterization of SARS-CoV-2 different variants and related morbidity and mortality: a systematic review. *European journal of medical research*. 2021 06;26(1):51-1. Available from: <https://pubmed.ncbi.nlm.nih.gov/34103090>.
186. Ingraham NE, Ingbar DH. The omicron variant of SARS-CoV-2: Understanding the known and living with unknowns. *Clinical and translational medicine*. 2021 12;11(12):e685-5. Available from: <https://pubmed.ncbi.nlm.nih.gov/34911167>.
187. Lou F, Li M, Pang Z, Jiang L, Guan L, Tian L, et al. Understanding the Secret of SARS-CoV-2 Variants of Concern/Interest and Immune Escape. *Frontiers in immunology*. 2021 11;12:744242-2. Available from: <https://pubmed.ncbi.nlm.nih.gov/34804024>.
188. Bhattacharya M, Sharma AR, Dhama K, Agoramoorthy G, Chakraborty C. Omicron variant (B.1.1.529) of SARS-CoV-2: understanding mutations in the genome, S-glycoprotein, and antibody-binding regions. *GeroScience*. 2022. Available from: <https://doi.org/10.1007/s11357-022-00532-4>.
189. Kissler SM, Fauver JR, Mack C, Tai CG, Breban MI, Watkins AE, et al. Viral Dynamics of SARS-CoV-2 Variants in Vaccinated and Unvaccinated Persons. *New England Journal of Medicine*. 2021;385(26):2489-91. Available from: <https://doi.org/10.1056/NEJMc2102507>.
190. Andreakos E, Abel L, Vinh DC, Kaja E, Drolet BA, Zhang Q, et al. A global effort to dissect the human genetic basis of resistance to SARS-CoV-2 infection. *Nature Immunology*. 2022;23(2):159-64. Available from: <https://doi.org/10.1038/s41590-021-01030-z>.
191. Doshi P. COVID-19: Do many people have pre-existing immunity? *BMJ*. 2020;370. Available from: <https://www.bmj.com/content/370/bmj.m3563>.
192. Castelli EC, de Castro MV, Naslavsky MS, Scliar MO, Silva NSB, Andrade HS, et al. "Immunogenetics of resistance to SARS-CoV-2 infection in discordant couples". *medRxiv*. 2021. Available from: <https://www.medrxiv.org/content/early/2021/04/25/2021.04.21.21255872>.
193. Nishiura H, Kobayashi T, Miyama T, Suzuki A, Jung SM, Hayashi K, et al. Estimation of the asymptomatic ratio of novel coronavirus infections (COVID-19). *Int J Infect Dis*. 2020 May;94:154-5.
194. Van Vinh Chau N, Lam VT, Dung NT, Yen LM, Minh NNQ, Hung LM, et al. The Natural History and Transmission Potential of Asymptomatic Severe Acute Respiratory Syndrome Coronavirus 2 Infection. *Clin Infect Dis*. 2020 Dec;71(10):2679-87.
195. Oran DP, Topol EJ. Prevalence of Asymptomatic SARS-CoV-2 Infection. *Annals of Internal Medicine*. 2020;173(5):362-7. PMID: 32491919. Available from: <https://doi.org/10.7326/M20-3012>.
196. Johansson MA, Quandelacy TM, Kada S, Prasad PV, Steele M, Brooks JT, et al. SARS-CoV-2 Transmission From People Without COVID-19 Symptoms. *JAMA network open*. 2021 01;4(1):e2035057-7. Available from: <https://pubmed.ncbi.nlm.nih.gov/33410879>.
197. Ellinghaus D, Degenhardt F, Bujanda L, Buti M, Albillos A, Invernizzi P, et al. Genomewide Association Study of Severe COVID-19 with Respiratory Failure. *N Engl J Med*. 2020 Oct;383(16):1522-34.

198. Buitrago-Garcia D, Egli-Gany D, Counotte MJ, Hossmann S, Imeri H, Ipekci AM, et al. Occurrence and transmission potential of asymptomatic and presymptomatic SARS-CoV-2 infections: A living systematic review and meta-analysis. *PLOS Medicine*. 2020 09;17(9):1-25. Available from: <https://doi.org/10.1371/journal.pmed.1003346>.
199. Killingley B, Mann AJ, Kalinova M, Boyers A, Goonawardane N, Zhou J, et al. Safety, tolerability and viral kinetics during SARS-CoV-2 human challenge in young adults. *Nature Medicine*. 2022. Available from: <https://doi.org/10.1038/s41591-022-01780-9>.
200. Mizumoto K, Kagaya K, Zarebski A, Chowell G. Estimating the asymptomatic proportion of coronavirus disease 2019 (COVID-19) cases on board the Diamond Princess cruise ship, Yokohama, Japan, 2020. *Eurosurveillance*. 2020;25(10). Available from: <https://www.eurosurveillance.org/content/10.2807/1560-7917.ES.2020.25.10.2000180>.
201. Lavezzo E, Franchin E, Ciavarella C, Cuomo-Dannenburg G, Barzon L, Del Vecchio C, et al. Suppression of a SARS-CoV-2 outbreak in the Italian municipality of Vo'. *Nature*. 2020 Aug;584(7821):425-9.
202. Moriarty LF, Plucinski MM, Marston BJ, Kurbatova EV, Knust B, Murray EL, et al. Public Health Responses to COVID-19 Outbreaks on Cruise Ships - Worldwide, February-March 2020. *MMWR Morb Mortal Wkly Rep*. 2020 Mar;69(12):347-52.
203. Walsh KA, Jordan K, Clyne B, Rohde D, Drummond L, Byrne P, et al. SARS-CoV-2 detection, viral load and infectivity over the course of an infection. *J Infect*. 2020 Sep;81(3):357-71.
204. McEvoy D, McAloon C, Collins A, Hunt K, Butler F, Byrne A, et al. Relative infectiousness of asymptomatic SARS-CoV-2 infected persons compared with symptomatic individuals: a rapid scoping review. *BMJ Open*. 2021;11(5). Available from: <https://bmjopen.bmj.com/content/11/5/e042354>.
205. Atkinson B, Petersen E. SARS-CoV-2 shedding and infectivity. *Lancet*. 2020 Apr;395(10233):1339-40.
206. Singanayagam A, Patel M, Charlett A, Lopez Bernal J, Saliba V, Ellis J, et al. Duration of infectiousness and correlation with RT-PCR cycle threshold values in cases of COVID-19, England, January to May 2020. *Eurosurveillance*. 2020;25(32). Available from: <https://www.eurosurveillance.org/content/10.2807/1560-7917.ES.2020.25.32.2001483>.
207. Lee S, Kim T, Lee E, Lee C, Kim H, Rhee H, et al. Clinical Course and Molecular Viral Shedding Among Asymptomatic and Symptomatic Patients With SARS-CoV-2 Infection in a Community Treatment Center in the Republic of Korea. *JAMA Internal Medicine*. 2020 11;180(11):1447-52. Available from: <https://doi.org/10.1001/jamainternmed.2020.3862>.
208. Uhm JS, Ahn JY, Hyun J, Sohn Y, Kim JH, Jeong SJ, et al. Patterns of viral clearance in the natural course of asymptomatic COVID-19: Comparison with symptomatic non-severe COVID-19. *Int J Infect Dis*. 2020 Oct;99:279-85.
209. He X, Lau EHY, Wu P, Deng X, Wang J, Hao X, et al. Temporal dynamics in viral shedding and transmissibility of COVID-19. *Nature Medicine*. 2020;26(5):672-5. Available from: <https://doi.org/10.1038/s41591-020-0869-5>.
210. Long QX, Tang XJ, Shi QL, Li Q, Deng HJ, Yuan J, et al. Clinical and immunological assessment of asymptomatic SARS-CoV-2 infections. *Nature Medicine*. 2020;26(8):1200-4. Available from: <https://doi.org/10.1038/s41591-020-0965-6>.